ImageJ software version 1.34s (National Institute of Health; NIH, USA).

Gelatine zymography

Supernatant media from monolayer and 3D collagen gel cultures (500 μL per culture condition) were concentrated 10-fold by precipitation with cold ethanol and re-suspended in 50 μL double-distilled H_2O. Gelatine zymography was performed by a modification of previously published procedures [20, 23, 24]. Briefly, 25 μL of each sample were separated in 10% SDS–PAGE containing 0.1% gelatine (Invitrogen, Carlsbad, CA, USA) under nonreducing conditions. After electrophoresis, the gels were soaked in 2.5% Triton-X 100 and incubated in metalloproteinase activation buffer containing $CaCl_2$ and $ZnCl_2$ for 16 h at 37°C. The gels were stained with 0.4% Coomassie blue (Bio-Rad) and rapidly destained with destaining buffer (30% methanol, 10% acetic acid). The gels were dried between cellophane sheets (Amersham, Piscataway, NJ, USA). Zones of proteolysis appeared as clear bands against a blue background and were scanned by Gel Doc 2000 (Bio-Rad). Band intensity was quantified using ImageJ software.

RNA preparation and complementary DNA synthesis

To determine whether changes in MMP mRNA levels were present, quantitative real-time PCR was performed. HFL-1 fibroblasts were cultured in 60-mm dishes at 1.5×10^6 cells for 24 h. Cells were then washed by PBS twice and treated with statins for 1 h before the stimulation by cytokines (TNF-α 5 $ng \cdot mL^{-1}$ and IL-1β 2 $ng \cdot mL^{-1}$) in SF-DMEM for 6 h. Total RNA was isolated by a single-step guanidinium–thiocyanate–phenol–chloroform extraction procedure designed by CHOMCYNSKI and SACCHI [25], and the total amount of RNA was quantified spectrophotometrically (Shimadzu Scientific Instruments, Inc., Columbia, MD, USA). 1 μg of total RNA was transcribed according to the previously published methods [20, 24].

Quantitative real-time PCR

Gene expression was measured with the use of an ABI Prism 7500 Sequence Detection System (Applied Biosystems) by a slight modification of previously published methods [20, 26]. The same primers and probes for MMP-1, -3 and -9 were used as described by FANG *et al.* [20]. rRNA was simultaneously tested using TaqMan Ribosomal RNA Control Reagents (Applied Biosystems).

Cell viability assay

Cell viability was evaluated by MTT assay using previously described methods [27]. Cells were treated with various concentrations of reagents used in this study with MTT solution at a final concentration of 1 $mg \cdot mL^{-1}$ for 6 h at 37°C. After incubation, dimethyl sulfoxide was added into each well. The absorbance of each sample at 540 nm was determined by BenchMark Microplate Reader (Bio-Rad).

Statistical analysis

Data are expressed as mean±SEM. Each experiment was repeated at least three times. The number of replicates is specified in each figure. Experiments with multiple comparisons were evaluated by one-way ANOVA followed by *post hoc* analysis by pairwise comparisons of values with Tukey's test to adjust for multiple comparisons. Probability p-values <0.05 were considered significant.

RESULTS

Effect of statins on MMP release in monolayer culture

HFL-1 cells

To test if statins inhibit the release of MMPs in HFL-1, we first investigated three separate statins, not only to demonstrate the reproducibility of our findings, but to be certain that any effects observed were not specific for a single compound. To accomplish this, cells were cultured in 60-mm dishes and treated with atorvastatin (2.5 μM), fluvastatin (1.0 μM) or simvastatin (0.5 μM) with and without stimulation by cytokines (TNF-α 5 $ng \cdot mL^{-1}$ and IL-1β 2 $ng \cdot mL^{-1}$) for 24 h. These concentrations of statins were chosen as they are considered to be close to those detected in the human body when administered therapeutically. Supernatants from each culture condition were assessed for MMP-1 and -3 release by Western blot analysis, and for MMP-2 and -9 by gelatine zymography. As expected, the cytokines stimulated MMP-1 and -3 release (fig. 1a–d). Bands corresponding to the latent forms (55 kDa) were observed, but lower molecular weight bands corresponding to active MMPs were not observed. All three statins inhibited both MMP-1 (fig. 1a and b) and MMP-3 (fig. 1c and d) release stimulated by cytokines ($p<0.05$ compared with the cytokine-treated controls). In monolayer culture, MMP-9 release was not observed under any condition. However, HFL-1 cells released a gelatinase corresponding to the latent form of MMP-2 (fig. 1e and f). The effect of atorvastatin on the release of the latent form of MMP-2 stimulated by cytokines was modest (fig. 1e and f). None of the reagents affected cell viability evaluated by MTT assay (data not shown).

To determine whether the inhibition of MMP-1 and -3 expression by atorvastatin was associated with changes in gene expression, quantitative real-time PCR was performed after 6 h of incubation with statins and cytokines (TNF-α 5 $ng \cdot mL^{-1}$ and IL-1β 2 $ng \cdot mL^{-1}$). Atorvastatin alone slightly stimulated both MMP-1 (fig. 2a) and MMP-3 (fig. 2b) mRNA expression. However, this effect was modest compared with that of the cytokines, which stimulated MMP-1 and -3 mRNA 121.6±3.8- and 46.9±1.0-fold of control, respectively. When cells were treated with atorvastatin before the stimulation by cytokines, the effect of the cytokines on both MMP-1 and -3 mRNA was inhibited to 12.3±1.4- and 7.1±0.4-fold of control, respectively ($p<0.01$ compared with the cytokine treated groups). Consistent with the results observed with gelatine zymography, no MMP-9 mRNA was detected (data not shown).

Adult lung fibroblasts

Because fibroblasts may be functionally heterogeneous, we also investigated the effect of atorvastatin on the inhibition of MMP release from normal adult human lung fibroblasts (HLF) after 24 h of culture. In contrast to HFL-1 cells, which did not release any detectable MMP-1 or -3 under control conditions, HLF cells released a small amount of MMP-1 and -3 corresponding in molecular size to the latent form of 55 kDa (online supplementary material fig. 1). As with HFL-1 cells, the cytokines also stimulated both MMP-1 and -3 release from HLF cells (online supplementary material fig. 1a–d). Also, as with HFL-1 cells, atorvastatin inhibited HLF release of both

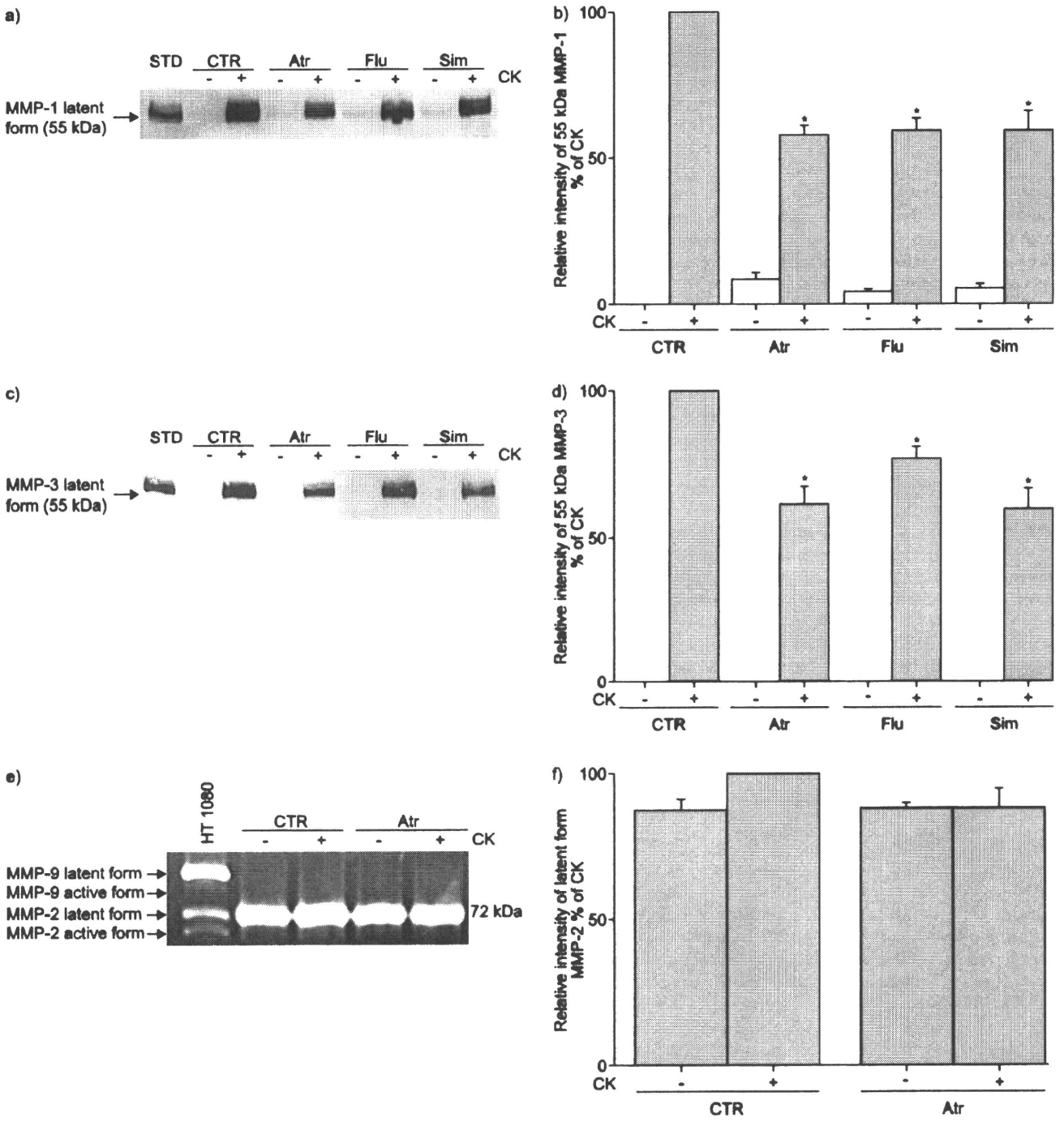

FIGURE 1. Effect of statins on matrix metalloproteinase (MMP) release by fibroblasts in monolayer culture. Human fetal lung fibroblast-1 cells cultured in monolayer were treated with atorvastatin (Atr; 2.5 μM), fluvastatin (Flu; 1.0 μM) and simvastatin (Sim; 0.5 μM). 1 h later, cytokines (CK; tumour necrosis factor-α 5 ng·mL^{-1} and interleukin-1α 2 ng·mL^{-1}) were added. Supernatant media harvested after 24 h were subjected to Western blot analysis for MMP-1 and MMP-3, and gelatine zymography for MMP-2 and MMP-9. a) MMP-1 western blot. The band corresponding to the latent form is indicated by the arrow. b) Quantification of MMP-1 staining. c) MMP-3 western blot. The band corresponding to the latent form of MMP-3 is indicated by the arrow. d) Quantification of MMP-3 staining. e) Gelatine zymography for MMP-2 and MMP-9. f) Quantification of MMP-2 staining. Densitometry data are shown as mean±SEM from three separate experiments performed on different occasions. STD: MMP-1 and MMP-3 standards; CTR: control; HT1080: supernatant from HT1080 cell monolayer culture as a positive control. *: $p<0.05$ compared with the cytokine-treated controls.

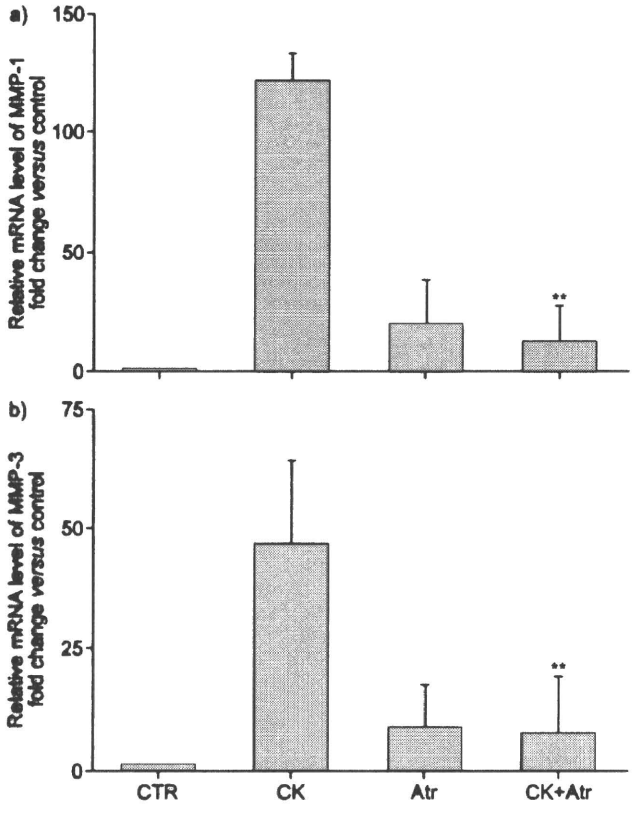

FIGURE 2. Effect of atorvastatin (Atr) on a) matrix metalloproteinase (MMP)-1 and b) MMP-3 mRNA expression. Human fetal lung fibroblast-1 fibroblasts cultured in monolayer were treated with and without atorvastatin (2.5 μM). 1 h later, cytokines (CK; tumour necrosis factor-α 5 ng·mL^{-1} and interleukin-1α 2 ng·mL^{-1}) were added and then cultured for 6 h. mRNA levels were quantified by Taqman RT-PCR. The vertical axes show mRNA expression level normalised to the amount of rRNA and expressed as fold of control. The data presented are mean±SEM from three separate experiments, each performed in duplicate. CTR: control. **: $p<0.01$ compared with cytokine treated groups.

MMP-1 (online supplementary material fig. 1a and b) and MMP-3 (online supplementary material fig. 1c and d) release stimulated by cytokines ($p<0.05$ compared with the cytokine-treated controls). The release of MMP-2 was similar to that of HFL-1 cells and, as with HFL-1 cells, MMP-9 was not detected in the supernatant of HLF cells in monolayer cultures (online supplementary material fig. 1e and f).

Role of the mevalonate pathway

Inhibition of MMP-1 and MMP-3 protein release

Incubation of cells with HMG-CoA reductase inhibitors, such as the statins, blocks production of mevalonate [28, 29]. Mevalonate metabolism yields a series of isoprenoids, including FPP and GGPP. To confirm that this is the pathway by which atorvastatin inhibits MMP-1 and -3 release, we tested whether mevalonate, FPP or GGPP could reverse atorvastatin inhibition of cytokine-stimulated HFL-1 MMP-1 and -3 release. HFL-1 cells were cultured in monolayer and treated with atorvastatin (2.5 μM) with or without mevalonate (100 μM), FPP (5 μM) or GGPP (5 μM) followed by stimulation with cytokines (TNF-α 5 ng·mL^{-1} and IL-1β 2 ng·mL^{-1}) for 24 h. In the presence of mevalonate, GGPP or FPP alone, there was no detectable level of MMP-1 release (fig. 3a) and this corresponded to the results under control conditions (data not shown). The addition of mevalonate and GGPP almost completely blocked the inhibitory effect of atorvastatin on the release of MMP-1 (fig. 3a and b; $p<0.05$ compared with cytokine-treated groups after incubation with atorvastatin). In contrast, FPP had no effect.

No MMP-3 was detected when cells were incubated under control conditions (data not shown) or with mevalonate, GGPP or FPP added alone (fig. 3c). Mevalonate and GGPP blocked the inhibitory effect of atorvastatin on MMP-3 release that was stimulated by cytokines (fig. 3c and d; $p<0.05$ compared with cytokine-treated groups after incubation with atorvastatin). FPP was without effect.

Inhibition of MMP-1 and MMP-3 mRNA expression

To determine whether the effects of mevalonate and GGPP were associated with changes in gene expression, quantitative real-time PCR assay was performed. HFL-1 cells were treated with atorvastatin (2.5 μM) with or without mevalonate (100 μM) or GGPP (5 μM), and then stimulated with cytokines (TNF-α 5 ng·mL^{-1} and IL-1β 2 ng·mL^{-1}) for 6 h. Neither mevalonate nor GGPP alone altered MMP-1 or -3 mRNA expression levels (fig. 4a and b, respectively; $p<0.01$ compared with cytokines plus atorvastatin treated groups). However, the addition of mevalonate or GGPP blocked the inhibitory effect of atorvastatin on MMP-1 and -3 mRNA expression significantly (fig. 4a and b, respectively). FPP did not have any effect on MMP-1 or -3 mRNA expression (data not shown).

Culture in 3D collagen gels

Effect of atorvastatin on collagen degradation

The response of fibroblasts to exogenously added mediators can vary depending on the culture condition. In 3D cultures in floating collagen gels, which are thought to more closely mimic *in vivo* conditions, we have previously shown that stimulation of fibroblasts with cytokines in the presence of NE can result in degradation of the collagen gel matrix [19]. To determine if atorvastatin inhibition of fibroblast MMP release could lead to inhibition of matrix degradation, we prepared 3D collagen gels populated with HFL-1 fibroblasts. When stimulated by cytokines (TNF-α 5 ng·mL^{-1} and IL-1β 2 ng·mL^{-1}) to induce MMP release in the presence of NE (10 nM), which leads to activation of MMPs, the collagen gels were degraded as we have reported previously [19]. The hydroxyproline content of the gels was significantly reduced after 3 days (hydroxyproline content 38±4% of control (fig. 5); $p<0.05$ compared with control). This decrease was almost completely inhibited by atorvastatin (hydroxyproline content 83±8% of control (fig. 5); $p<0.05$ compared with cytokine + NE). Hydroxyproline content of gels treated with atorvastatin + cytokines (without NE) or atorvastatin + NE (without cytokines) was the same as that of control (data not shown).

Effect of atorvastatin on MMP release

To confirm the results obtained in monolayer culture on plastic, we also assessed the effect of atorvastatin on MMP release in 3D culture in collagen gels. There were modest

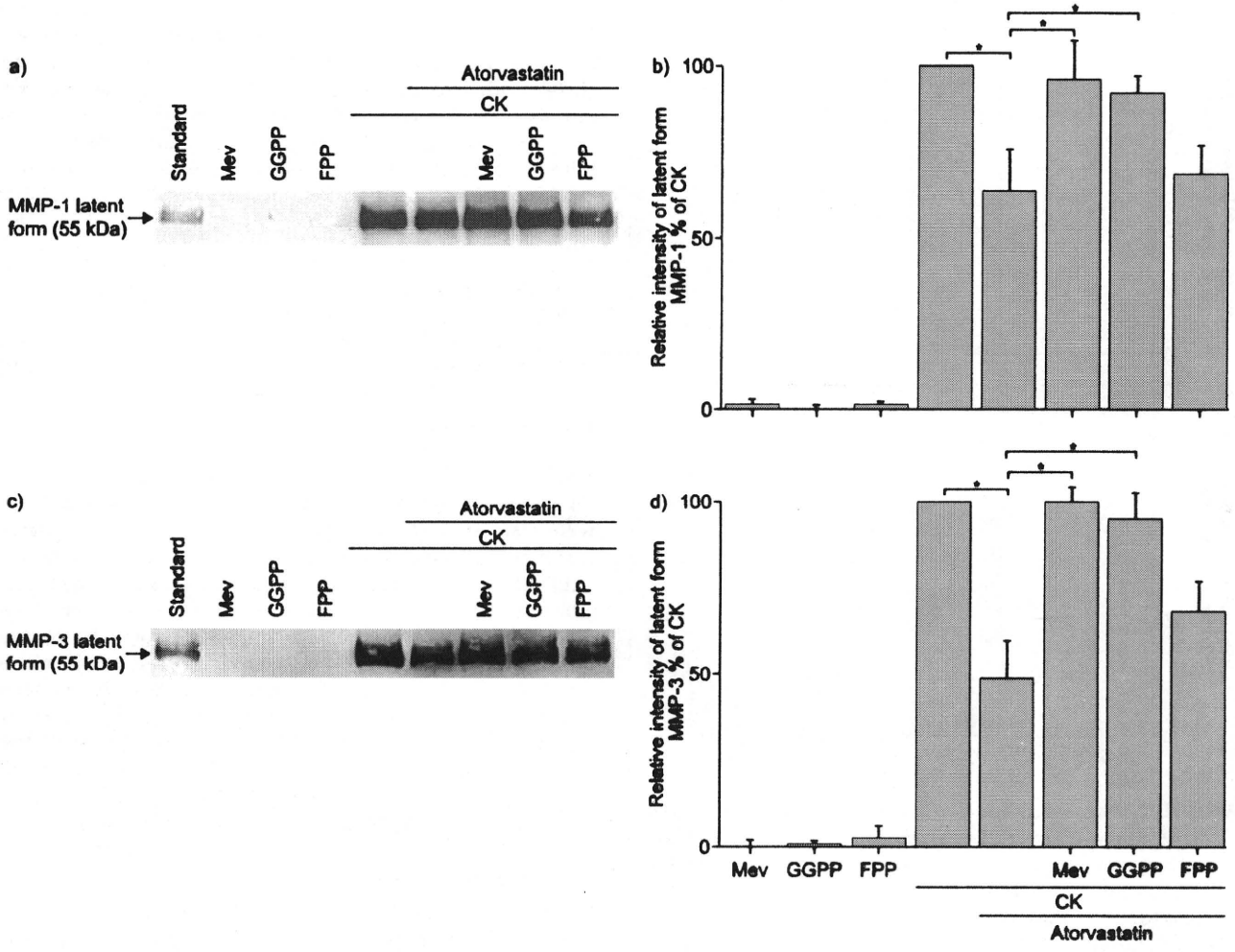

FIGURE 3. Effect of mevalonate (Mev) and isoprenoids on atorvastatin inhibition of a) MMP-1 and b) MMP-3 release. Human fetal lung fibroblast-1 cells were cultured in monolayer and treated with atorvastatin (2.5 μM) with or without Mev, geranylgeranyl pyrophosphate (GGPP) or farnesyl pyrophosphate (FPP). 1 h later, cytokines (CK; tumour necrosis factor-α 5 ng·mL^{-1} and interleukin-1α 2 ng·mL^{-1}) were added. Supernatant media harvested after 24 h were subjected to Western blot analysis for MMP-1 and MMP-3. a) MMP-1 and c) MMP-3 Western blots. The band corresponding to the latent form is indicated by the arrow. Quantification of b) MMP-1 and d) MMP-3 staining. Densitometry data are shown as mean ± SEM for three separate experiments performed on separate occasions. *: $p<0.05$.

differences in MMP release under control conditions. For example, detectable MMP-1 was released in latent form under control conditions in 3D culture, which contrasts with the undetectable levels in monolayer culture. Importantly, as with monolayer culture, there was marked increase in release of MMP-1 following cytokine stimulation (online supplementary material fig. 2). As in monolayer culture, MMP-3 was undetectable under control conditions in 3D culture (online supplementary material fig. 3). MMP-2, which was released in the latent form in monolayer culture, was released in both latent and active forms under control conditions in 3D culture (online supplementary material fig. 4). MMP-9, which was not released under any conditions tested in monolayer culture, was not released under control conditions in 3D culture, but its release was stimulated by cytokines (TNF-α 5 ng·mL^{-1} and IL-1α 2 ng·mL^{-1}) (online supplementary material fig. 4). Importantly, the cytokines stimulated the release of all the MMPs assessed, MMP-1, -3 and -9, and this release was inhibited ($p<0.05$ compared with cytokines) in all cases by atorvastatin (online supplementary material figs 2, 3 and 4). There was, moreover, a reduction in the conversion of latent MMPs to the active forms in the presence of NE for MMP-1 ($p<0.05$), -3 ($p<0.01$) and -9 ($p<0.001$). A modest effect, which was not quantified, was also observed in inhibiting MMP-2 release (online supplementary material fig. 4a).

Role of the mevalonate pathway in inhibition of collagen gel degradation

To confirm that atorvastatin inhibited collagen gel degradation by the same pathway by which it inhibited MMP release in monolayer culture, we assessed the ability of mevalonate (100 μM), FPP (5 μM) and GGPP (5 μM) to block atorvastatin inhibition of collagen gel degradation induced by the combination of cytokines and NE. After 3 days of culture in the presence of cytokines and NE, collagen gel hydroxyproline content was reduced by more than half (online supplementary

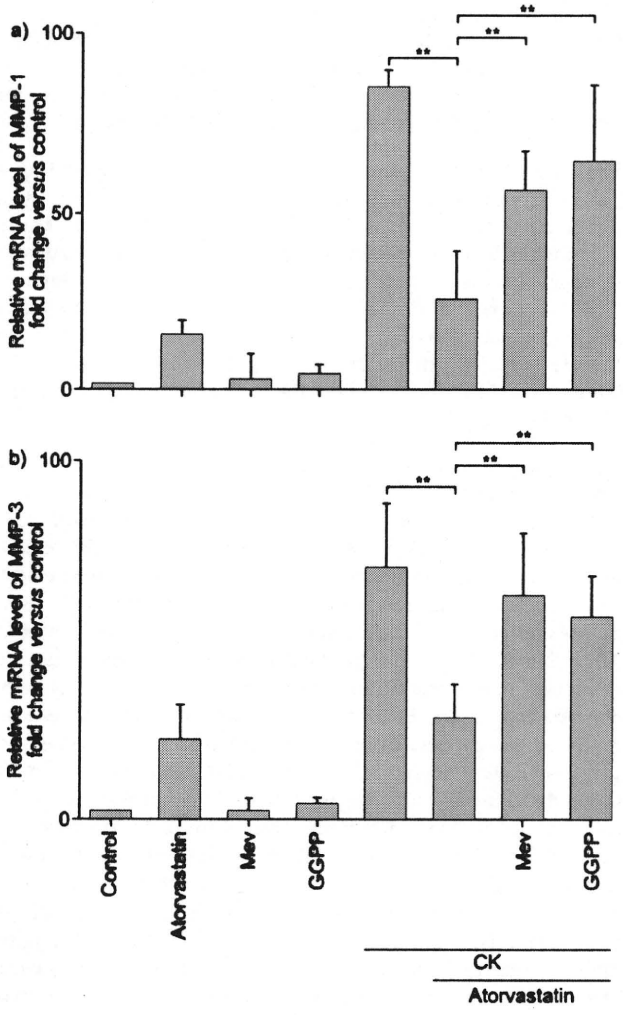

FIGURE 4. Effect of mevalonate (Mev) and isoprenoids on atorvastatin inhibition of a) matrix metalloproteinase (MMP)-1 and b) MMP-3 mRNA expression. Human fetal lung fibroblast-1 cells were cultured in monolayer and treated with atorvastatin (2.5 μM) with or without Mev or geranylgeranyl pyrophosphate (GGPP). 1 h later, cytokines (CK; tumour necrosis factor-α 5 ng·mL^{-1} and interleukin-1α 2 ng·mL^{-1}) were added and cultured for 6 h. mRNA levels were quantified by Taqman RT-PCR. Vertical axes show the mRNA expression level normalised to the amount of rRNA and expressed as fold of control. The data presented are mean±SEM from three separate experiments, each performed in duplicate. **: $p<0.01$.

material fig. 5; $p<0.05$ compared with control), indicating degradation of the collagen gels. Atorvastatin almost completely inhibited this degradation ($p<0.05$ compared with cytokines + NE). Mevalonate and GGPP had no effect when added alone, but almost completely reversed atorvastatin inhibition of collagen degradation caused by cytokines and NE (fig. 3; $p<0.05$ compared with control). In contrast, FPP had no effect when added alone and did not reverse the inhibitory effect of atorvastatin on collagen gel degradation.

Role of the mevalonate pathway in 3D culture

Because fibroblasts in 3D culture release MMP somewhat differently than in monolayer culture, we also investigated

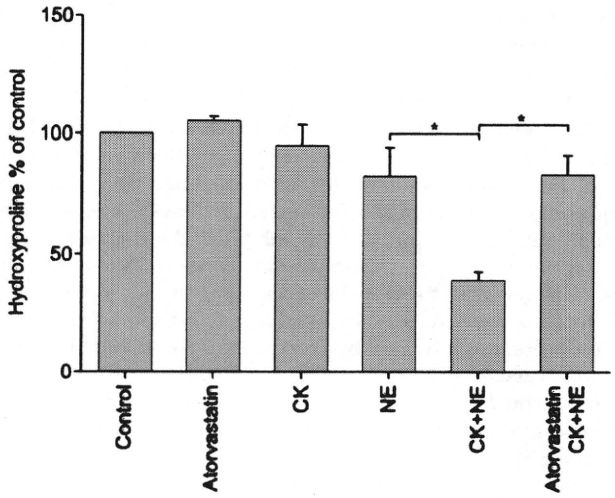

FIGURE 5. Effect of atorvastatin on collagen gel degradation induced by cytokines (CK) together with neutrophil elastase (NE). Human fetal lung-1 fibroblasts (3×10^5 cells·mL^{-1}) were cast into three-dimensional collagen gels and released into floating media (serum-free Dulbecco's modified Eagle's medium) containing atorvastatin (2.5 μM). 1 h later, CK (tumour necrosis factor-α 5 ng·mL^{-1} and interleukin-1α 2 ng·mL^{-1}) were added; NE was added the next day. The gels were cultured for three more days and hydroxyproline content in the gels was determined. The data presented are mean±SEM from three separate experiments, each of which included triplicate gels for each condition. *: $p<0.05$.

whether mevalonate or isoprenoids blocked the effect of atorvastatin on MMP release in 3D gel culture (online supplementary material fig. 6). Although statistical significance was not achieved, there was a trend for both mevalonate and GGPP to block the inhibitory effect of atorvastatin on the amount of detectable active MMP-1 released in the presence of cytokines and NE (online supplementary material fig. 6a and b). Both mevalonate and GGPP significantly blocked the inhibitory effect of atorvastatin on MMP-3 release (online supplementary material fig. 6c and d; $p<0.01$) and on the release of MMP-9 and its conversion to an 84 kDa size that corresponds to the active form MMP-9 (online supplementary material fig. 6e and f; $p<0.01$). FPP was consistently without effect.

Adult HLF in 3D culture

Collagen degradation

To confirm that collagen gel degradation occurs in the gels populated with adult HLF and that MMP release by these cells is also blocked by atorvastatin, cultured HLF cells were cast into 3D cultures and treated with cytokines and NE to induce degradation. As observed with HFL-1 cells, in the presence of cytokines and NE, hydroxyproline content of the gels was significantly reduced after 3 days of culture (online supplementary material fig. 7; $p<0.05$ compared with control). This decrease was inhibited by atorvastatin ($p<0.05$ compared with cytokines + NE). The role of the mevalonate pathway also appeared to be the same in HLF cells, as mevalonate and GGPP had no effect when added alone, but reversed the effect of atorvastatin on the inhibition of collagen degradation caused by cytokines and NE (online supplementary material fig. 7; $p<0.05$ compared with control).

DISCUSSION

The current study demonstrates that HMG-CoA reductase inhibitors can inhibit cytokine-induced release of MMPs from human lung fibroblasts cultured in both monolayer and 3D collagen gels. Release of both MMP-1 and -3 from fibroblasts in monolayer culture was inhibited by atorvastatin, simvastatin and fluvastatin. Atorvastatin also inhibited the cytokine-induced expression of MMP-1 and MMP-3 mRNA expression. In 3D gel culture, atorvastatin inhibited the degradation of collagen gels that was induced by cytokines in the presence of NE. In contrast to monolayer culture, in 3D gel culture, fibroblasts were induced by cytokines to release MMP-9, and these were also inhibited by atorvastatin. All of these changes were reversed by the addition of mevalonate and GGPP, which are intermediates in the HMG-CoA reductase pathway that bypass the step inhibited by statins. Interestingly, the intermediate FPP did not reverse these effects of atorvastatin. Taken together, the current data suggest that statins may modulate remodelling processes mediated by lung fibroblasts by inhibiting the release of MMPs.

Since the classic studies of LAURELL and ERIKSSON [30], proteases have been believed to play a major role in the pathogenesis of COPD. In particular, the MMPs have been suggested to play a prominent role. In support of this concept, mice deficient in the macrophage elastase MMP-12 have been reported to be resistant to the development of cigarette smoke-induced emphysema [31], although MMP-12 is not prominent in human emphysema [32]. Increased MMP-9 expression in the lungs has been reported to be associated with emphysema, in both experimental [33–37] and clinical [38] studies. Moreover, immunohistochemical analysis of COPD lungs showed an increased expression of collagenase 1 (MMP-1) and collagenase 2 (MMP-8) [39], and alveolar epithelial cells from patients with emphysema express MMP-1 mRNA and protein, and exhibit collagenase activity [40].

MMPs are expressed in low to undetectable levels in normal lung, but are readily detected in many lung diseases in addition to emphysema. In this context, the expression of MMPs is not restricted to inflammatory cells; virtually all cells, including alveolar epithelial cells and fibroblasts, can make MMPs [40, 41]. Alveolar fibroblasts, which comprise ~40% of alveolar cells [42], are believed to be the major cells responsible for the production and remodelling of ECM. They are one of the major sources of MMPs, which are secreted following lung injury. Therefore, inhibition of MMP release from fibroblasts could confer a new therapeutic approach to prevent the lung destruction observed in emphysema. Whether inhibition by statins could lead to toxicities, *e.g.* by inhibiting lung tissue turnover in fibrotic areas, of course, is a potential toxicity that would need to be considered.

Statins were originally developed for their cholesterol-lowering properties and efficacy in cardiovascular disease. However, evidence of pleiotropic effects of statins has been accumulating and suggests immunomodulatory, antioxidant, antithrombogenic and vascular actions [7, 29]. Several statins have been reported to inhibit the expression of MMPs in vascular cells and macrophages *in vitro* [9–11]. Consistent with this effect on MMPs, statins have been reported to inhibit the development of emphysema in model systems. In a rat model of cigarette smoking-induced emphysema, LEE *et al.* [43] found that simvastatin inhibited lung parenchymal destruction and MMP-9 expression. In a mouse model of emphysema induced by elastase, simvastatin reduced mRNA expression for interferon-γ, TNF-α and MMP-12 in the whole lung [44].

The current study extends these observations by providing a basis for statins to alter lung structural remodelling by a direct effect on fibroblast MMP release. Further, our study demonstrates that the effect of the statins is mediated through the mevalonate pathway, which is likely to involve GGPP but not FPP. This observation is similar to other studies, which also observed that the addition of FPP did not reverse the effect of statins [45, 46]. The mechanism for the failure of FPP to reverse these statin effects remains unexplained.

As with the normal lung, fibroblasts in culture release very low amounts of MMP-1, -2, -3 and -9. The release of these MMPs, however, can be readily induced by the inflammatory cytokines TNF-α + IL-1β, and it is the induced MMP release that statins were demonstrated to inhibit in the current study. This inhibition occurred both in the more conventionally used monolayer culture system (on plastic dishes) and in culture in 3D collagen gels, a system that is believed to more closely resemble tissue conditions [14, 16, 47]. In this system, degradation of the ECM can be quantified, and statins also inhibited this process. Some modest differences were observed between cells grown in monolayer and 3D culture. Part of these differences could be related to MMP retention in the collagen gel in the 3D system. This is unlikely, however, to account for the production of MMP-9 in 3D culture, which was not observed in monolayer culture. While there were some differences between the culture systems, the consistency of the inhibitory effects of statins, which were also observed in both the fetal strain of fibroblasts HFL-1 that has been widely used to explore lung fibroblast biology and in a strain of normal adult fibroblasts, suggests that the inhibitory effects of statins are robust.

In the current study, statins slightly increased the release of MMP-1 when added alone, and this was confirmed at both the mRNA and protein levels. Atorvastatin also slightly increased MMP-3 mRNA when added alone; however, MMP-3 was not detected at the protein level. The mechanisms that lead to mild stimulation when added alone and marked inhibition when added together with cytokines are unclear, but similar effects have been observed in other regulatory networks when agents can have multiple effects. These observations, therefore, suggest that statins might be modulating MMP release at several levels.

In summary, the current study demonstrates that statins can inhibit MMP release from HLFs in both monolayer and 3D collagen gel cultures. This effect is mediated through the inhibition of the HMG-CoA reductase pathway. Through actions on fibroblast MMP release, statins may modulate remodelling processes mediated by fibroblasts. The use of statins, therefore, may have therapeutic potential in diseases characterised by alterations in tissue architecture, particularly diseases characterised by tissue destruction, such as emphysema.

SUPPORT STATEMENT
Funded by a grant from Pfizer Pharmaceuticals.

STATEMENT OF INTEREST
A statement of interest for S.I. Rennard, and this study itself can be found at www.erj.ersjournals.com/misc/statements.dtl

ACKNOWLEDGEMENTS
The authors thank the excellent secretarial support of L. Richards.

REFERENCES

1 Murray CJ, Lopez AD. Alternative projection of mortality by cause 1990–2020: global burden of disease study. *Lancet* 1997; 349: 1498–1504.
2 World Health Organization, Global strategy for diagnosis, management and prevention of COPD, 2007. www.goldcopd.com Date last updated: January, 2009. Date last accessed: November 30, 2009.
3 Mancini GB, Etminan M, Zhang B, *et al.* Reduction of morbidity and mortality by statins, angiotensin-converting enzyme inhibitors, and angiotensin receptor blockers in patients with chronic obstructive pulmonary disease. *J Am Coll Cardiol* 2006; 47: 2554–2560.
4 Ishida W, Kajiwara T, Ishii M, *et al.* Decrease in mortality rate of chronic obstructive pulmonary disease (COPD) with statin use: a population-based analysis in Japan. *Tohoku J Exp Med* 2007; 212: 265–273.
5 Soyseth V, Brekke PH, Smith P, *et al.* Statin use is associated with reduced mortality in COPD. *Eur Respir J* 2007; 29: 279–283.
6 Keddissi JI, Younis WG, Chbeir EA, *et al.* The use of statins and lung function in current and former smokers. *Chest* 2007; 132: 1764–1771.
7 Bonetti PO, Lerman LO, Napoli C, *et al.* Statin effects beyond lipid lowering – are they clinically relevant? *Eur Heart J* 2003; 24: 225–248.
8 Hothersall E, McSharry C, Thomson NC. Potential therapeutic role for statins in respiratory disease. *Thorax* 2006; 61: 729–734.
9 Ikeda U, Shimpo M, Ohki R, *et al.* Fluvastatin inhibits matrix metalloproteinase-1 expression in human vascular endothelial cells. *Hypertension* 2000; 36: 325–329.
10 Bellosta S, Via D, Canavesi M, *et al.* HMG-CoA reductase inhibitors reduce MMP-9 secretion by macrophages. *Arterioscler Thromb Vasc Biol* 1998; 18: 1671–1678.
11 Luan Z, Chase AJ, Newby AC. Statins inhibit secretion of metalloproteinases-1, -2, -3, and -9 from vascular smooth muscle cells and macrophages. *Arterioscler Thromb Vasc Biol* 2003; 23: 769–775.
12 Parks WC, Shapiro SD. Matrix metalloproteinases in lung biology. *Respirat Res* 2001; 2: 10–19.
13 Hogg JC, Senior RM. Chronic obstructive pulmonary disease - part 2: pathology and biochemistry of emphysema. *Thorax* 2002; 57: 830–834.
14 Grinnell F. Fibroblasts, myofibroblasts and wound contraction. *J Cell Biol* 1994; 124: 401–404.
15 Breul SD, Bradley KH, Hance AJ, *et al.* Control of collagen production by human diploid lung fibroblasts. *J Biol Chem* 1980; 255: 5250–5260.
16 Elsdale T, Bard J. Collagen substrata for studies on cell behavior. *J Cell Biol* 1972; 54: 626–637.
17 Mio T, Adachi Y, Romberger DJ, *et al.* Regulation of fibroblast proliferation in three dimensional collagen gel matrix. *In vitro Cell Dev Biol* 1996; 32: 427–433.
18 Reddy GK, Enwemeka CS. A simplified method for the analysis of hydroxyproline in biological tissues. *Clin Biochem* 1996; 29: 225–229.
19 Zhu YK, Liu XD, Skold CM, *et al.* Synergistic neutrophil elastase-cytokine interaction degrades collagen in three-dimensional culture. *Am J Physiol Lung Cell Mol Physiol* 2001; 281: L868–L878.
20 Fang Q, Liu X, Al-Mugotir M, *et al.* Thrombin and TNF-α/IL-1β synergistically induce fibroblast-mediated collagen gel degradation. *Am J Respir Cell Mol Biol* 2006; 35: 714–721.
21 Henry MT, McMahon K, Mackarel AJ, *et al.* Matrix metalloproteinases and tissue inhibitor of metalloproteinase-1 in sarcoidosis and IPF. *Eur Respir J* 2002; 20: 1220–1227.
22 Kubo S, Kobayashi M, Masunaga Y, *et al.* Cytokine and chemokine expression in cigarette smoke-induced lung injury in guinea pigs. *Eur Respir J* 2005; 26: 993–1001.
23 Zhang Y, McCluskey K, Fujii K, *et al.* Differential regulation of monocyte matrix metalloproteinase and TIMP-1 production by TNF-alpha, granulocyte-macrophage CSF, and IL-1 β through prostaglandin-dependent and -independent mechanisms. *J Immunol* 1998; 161: 3071–3076.
24 Zhu YK, Liu XD, Sköld CM, *et al.* Collaborative interactions between neutrophil elastase and metalloproteinases in extracelullar matrix degradation in three-dimensional collagen gels. *Respir Res* 2001; 2: 300–305.
25 Chomczynski P, Sacchi N. Single-step method of RNA isolation by acid guanidine thiocyanate-phenol-chloroform extraction. *Anal Biochem* 1987; 162: 156–159.
26 Bustin SA. Absolute quantification of mRNA using real-time reverse transcription polymerase chain reaction assays. *J Mol Endocrinol* 2000; 25: 169–193.
27 Supino R. MTT assays. *Methods Mol Biol* 1995; 43: 137–149.
28 Goldstein JL, Brown MS. Regulation of the mevalonate pathway. *Nature* 1990; 343: 425–430.
29 Greenwood J, Steinman L, Zamvil SS. Statin therapy and autoimmune disease: from protein prenylation to immunomodulation. *Nat Rev Immunol* 2006; 6: 358–370.
30 Laurell CB, Eriksson S. The electrophoretic α 1-globulin pattern of serum in α 1-antitrypsin deficiency. *Scand J Clin Lab Invest* 1963; 15: 132–140.
31 Hautamaki RD, Kobayashi DK, Senior RM, *et al.* Requirement for macrophage elastase for cigarette smoke-induced emphysema in mice. *Science* 1997; 277: 2002–2004.
32 Finlay GA, O'Driscoll LR, Russell KJ, *et al.* Matrix metalloproteinase expression and production by alveolar macrophages in emphysema. *Am J Crit Care Med* 1997; 156: 240–247.
33 Selman M, Cisneros-Lira J, Gaxiola M, *et al.* Matrix metalloproteinases inhibition attenuates tobacco smoke-induced emphysema in Guinea pigs. *Chest* 2003; 123: 1633–1641.
34 Zheng T, Zhu Z, Wang Z, *et al.* Inducible targeting of IL-13 to the adult lung causes matrix metalloproteinase- and cathepsin-dependent emphysema. *J Clin Invest* 2000; 106: 1081–1093.
35 Choe KH, Taraseviciene-Stewart L, Scerbavicius R, *et al.* Methylprednisolone causes matrix metalloproteinase-dependent emphysema in adult rats. *Am J Respir Crit Care Med* 2003; 167: 1516–1521.
36 Taraseviciene-Stewart L, Scerbavicius R, Choe KH, *et al.* An animal model of autoimmune emphysema. *Am J Respir Crit Care Med* 2005; 171: 734–742.
37 Lappalainen U, Whitsett JA, Wert SE, *et al.* Interleukin-1β causes pulmonary inflammation, emphysema, and airway remodeling in the adult murine lung. *Am J Respir Cell Mol Biol* 2005; 32: 311–318.
38 Russell RE, Culpitt SV, DeMatos C, *et al.* Release and activity of matrix metalloproteinase-9 and tissue inhibitor of metalloproteinase-1 by alveolar macrophages from patients with chronic obstructive pulmonary disease. *Am J Respir Cell Mol Biol* 2002; 26: 602–609.

39 Segura-Valdez L, Pardo A, Gaxiola M, *et al.* Upregulation of gelatinases A and B, collagenases 1 and 2, and increased parenchymal cell death in COPD. *Chest* 2000; 117: 684–694.
40 Imai K, Dalal SS, Chen ES, *et al.* Human collagenase (matrix metalloproteinase-1) expression in the lungs of patients with emphysema. *Am J Respir Crit Care Med* 2001; 163: 786–791.
41 Shapiro SD, Senior RM. Matrix metalloproteinases. Matrix degradation and more. *Am J Respir Cell Mol Biol* 1999; 20: 1100–1102.
42 Crapo JD, Barry BE, Gehr P, *et al.* Cell number and cell characteristics of the normal human lung. *Am Rev Respir Dis* 1982; 126: 332–337.
43 Lee JH, Lee DS, Kim EK, *et al.* Simvastatin inhibits cigarette smoking-induced emphysema and pulmonary hypertension in rat lungs. *Am J Respir Crit Care Med* 2005; 172: 987–993.
44 Takahashi S, Nakamura H, Furuuchi M. Simvastatin suppresses the development of elastase-induced emphysema in mice (abstract). *Proc Am Thor Soc* 2005; 2: A135.
45 Watts KL, Spiteri MA. Connective tissue growth factor expression and induction by transforming growth factor-β is abrogated by simvastatin *via* a Rho signaling mechanism. *Am J Physiol Lung Cell Mol Physiol* 2004; 287: L1323–L1332.
46 Takeda N, Kondo M, Ito S, *et al.* Role of RhoA inactivation in reduced cell proliferation of human airway smooth muscle by simvastatin. *Am J Respir Cell Mol Biol* 2006; 35: 722–729.
47 Bell E, Ivarsson B, Merrill C. Production of a tissue-like structure by contraction of collagen lattices by human fibroblasts of different proliferative potential *in vitro*. *Proc Natl Acad Sci USA* 1979; 76: 1274–1278.

EXPERIMENTAL CELL RESEARCH 316 (2010) 3501–3511

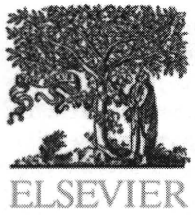

available at www.sciencedirect.com

ScienceDirect

www.elsevier.com/locate/yexcr

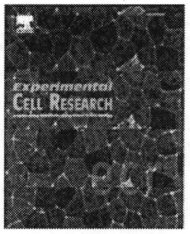

Research Article

Hepatic growth factor (HGF) inhibits cigarette smoke extract induced apoptosis in human bronchial epithelial cells☆

Shinsaku Togo[a,b], *Hisa Sugiura*[c], *Amy Nelson*[a], *Tetsu Kobayashi*[d], *Xingqi Wang*[a], *Koh Kamio*[e], *Shin Kawasaki*[f], *Peter Bitterman*[g], *Stephen I. Rennard*[a], *Xiangde Liu*[a,*]

[a]*Pulmonary, Critical Care, Sleep and Allergy Division, Department of Internal Medicine, University of Nebraska Medical Center, Omaha, NE, USA*
[b]*Department of Respiratory Medicine, Juntendo University School of Medicine, Tokyo, Japan*
[c]*Third Department of Internal Medicine, Wakayama Medical University, Wakayama, Japan*
[d]*Division of Pulmonary and Critical Care, The 3rd Department of Internal Medicine, Mie University Graduate School of Medicine, Mie, Japan*
[e]*Division of Pulmonary Medicine, Nippon Medical School, Tokyo, Japan*
[f]*Department of Respiratory Medicine, The University of Tokyo, Tokyo, Japan*
[g]*Department of Medicine, University of Minnesota, Minneapolis, MN, USA*

ARTICLE INFORMATION

Article Chronology:
Received 28 May 2010
Revised version received
25 August 2010
Accepted 9 September 2010
Available online 17 September 2010

Keywords:
HGF
Cigarette smoke extract
Apoptosis
DNA content

ABSTRACT

Low concentrations of cigarette smoke induced DNA damage and repair without leading to apoptosis in human bronchial epithelial cells. Higher concentrations of cigarette smoke, however, could induce either apoptosis or necrosis. The current study demonstrated that 15% cigarette smoke extract (CSE) induced apoptosis as evidenced by DNA content profiling ($17.8 \pm 2.1\%$ vs $10.2 \pm 1.6\%$ of control, $p < 0.05$), LIVE/DEAD staining ($60.2 \pm 2.1\%$ viable cells in CSE-treated vs $86.5 \pm 2.3\%$ in control cells, $p < 0.05$), and COMET assay ($24.3 \pm 0.6\%$ of Apoptotic Index in the cells treated with CSE vs $4.7 \pm 0.6\%$ of control, $P < 0.05$). Hepatocyte growth factor (HGF) significantly blocked the cigarette smoke-induced apoptosis as shown by DNA profiling ($10.8 \pm 1.5\%$ of CSE + HGF, $p < 0.05$), LIVE/DEAD staining ($78.5 \pm 1.2\%$ in CSE + HGF treated cells, $p < 0.05$), and COMET assay (Apoptotic Index: $10.0 \pm 0.8\%$ in CSE + HGF treated cells, $P < 0.05$). This protective effect of HGF on CSE-induced apoptosis was abolished by PI3K inhibitors, wortmannin and LY294002, and by introduction of the dominant negative AKT into the cells. Furthermore, CSE plus HGF could induce phosphorylation of AKT Thr 308 and the pro-apoptotic protein, BAD. These results suggest that HGF modulates cell survival in response to cigarette smoke exposure through the PI3K/AKT signaling pathway.

Introduction

Cigarette smoke is a major cause of chronic obstructive pulmonary disease (COPD) and lung cancer. Cigarette smoke contains as many as 6000 compounds and may damage the lungs through a variety of mechanisms. Nevertheless, the pathways by which cigarette smoke causes lung diseases remain incompletely defined. One major effect of cigarette smoke, however, is DNA damage and the time-dependent accumulation of somatic cell mutations in smokers. These mutations are believed to lead to altered cellular regulation and to contribute to the development of lung cancer. Similar mechanisms may contribute to the development of COPD [1,2].

☆ Disclosure of funding: Larson Endowment, University of Nebraska Medical Center.

* *Corresponding author.* 985910 Nebraska Medical Center, Omaha, Nebraska 68198-5910, USA. Fax: +1 402 559 4878.
E-mail address: xdliu@unmc.edu (X. Liu).

0014-4827/$ – see front matter © 2010 Elsevier Inc. All rights reserved.
doi:10.1016/j.yexcr.2010.09.006

Hepatocyte growth factor (HGF) is a peptide growth factor produced by mesenchymal cells that act on epithelial cells. The increased expression of HGF has been reported in cigarette smokers and has been associated with the development of lung cancer [3,4]. In addition, HGF appears to play an important role in the development of the lung and in the maintenance of the lung structure following injury [5–7]. In this context, HGF and its c-Met receptor play a role in normal post-natal alveolar wall formation and are up regulated following oxygen-induced lung injury [7]. Similarly, HGF plays a role in compensatory lung growth following pneumonectomy [8]. In addition, induced HGF expression has been reported to enhance alveolar regeneration following elastase and bleomycin injury in the mouse [9,10]. Conversely, decreased HGF production has been associated with pulmonary emphysema [11].

Several studies have demonstrated that the sensitivity of human bronchial epithelial cells to undergo apoptosis can be modulated by exogenous signals. In this context, cigarette smoke-induced signaling through the STAT3 and NF-κB pathways has been reported to inhibit apoptosis in the face of cigarette smoke-induced DNA damage [12,13]. The ability of HGF to modulate epithelial cell growth suggests that HGF might also modulate cigarette smoke-induced cytotoxicity through a mechanism of up-regulating anti-apoptotic pathways such as the AKT pathway. The current study was designed to evaluate this hypothesis.

Materials and methods

Materials

LHC basal medium, LHC-9 medium, RPMI 1640 medium, trypsin/EDTA, Dulbecco's Modified Eagle's Medium (DMEM), fetal calf serum (FCS), penicillin G sodium, and streptomycin were purchased from Invitrogen (Life Technologies, Grand Island, NY) and amphotericin B from Pharma-Tek (Elmira, NY). Vitrogen 100 was purchased from Cohesion Technologies (Palo Alto, CA). Hepatocyte growth factor (HGF), and caspases-3, -8, and -9 activity assay kits were purchased from R&D Systems (Minneapolis, MN). LY294002 was purchased from Cell Signaling Technology (Beverly, MA). Wortmannin, propidium iodide and camptothecin (CPT) were purchased from Sigma (St. Louis, MO). Rabbit anti-goat IgG horseradish peroxidase was purchased from Rockland Immunochemicals (Gilbertsville, PA).

Cell culture

Normal human bronchial epithelial cells (HBECs) were acquired from bronchial biopsies using a previously published method with modifications [14]. HBECs were cultured under serum-free conditions using a 1:1 mixture of LHC-9/RPMI 1640. Cells were plated on collagen (Vitrogen 30)-coated tissue culture dishes (Falcon; Becton-Dickinson Labware, Lincoln Park, NJ) at 37 °C in a humidified, 5% CO_2 atmosphere. Cells were passaged once a week at a 1:3 ratio. Cells between the 3rd and 10th passage were used for experiments.

Cigarette smoke extract preparation and dilution

Cigarette smoke extract (CSE) was prepared with a modification of the method of Carp and Janoff [15]. Briefly, one 100-mm cigarette without filter (Research Grade Cigarette, University of Kentucky) was combusted with a Variable Speed Pump (Fisher Scientific, Pittsburgh, PA). The smoke was bubbled through 25 ml double-distilled water (ddH2O) at a speed of 50 cc/min. The resulting suspension was filtered through a 0.22-μm-pore size filter (Lida Manufacturing Corp., Kenosha, WI) to remove bacteria and large particles. The pH of the CSE in the current study ranged from 7.34 to 7.40. This solution was considered to be 100% CSE and was diluted with LHC-D/RPMI 1640 medium within 30 min of preparation to obtain the desired concentration in each experiment. In the current study, 15% CSE was chosen in that 10% CSE or less caused only reversible DNA damage but not apoptosis [16], while over 20% CSE caused necrosis in HBECs.

Detection of cell viability and apoptosis

Live/dead assay

Cells were treated with various concentrations of CSE in the presence or absence of HGF or 1 μM CPT as a positive control for 24 h in 6-well plates. Cells were harvested with trypsin, combined with floating cells, and maintained in suspension in medium containing soybean trypsin inhibitor (STI). HBEC survival was quantified using a LIVE/DEAD Viability/Cytotoxicity kit (L-3224, Molecular Probes, Eugene, Oregon) in accordance with the manufacturer's protocol. The stained cells were cytospun, examined by epifluorescence microscopy (Nikon Eclipse E800; Nikon, Melville, NY) and photographed with a digital camera (Optronics, Goleta, CA) at 200× magnification. HBEC viability was determined by examining five random fields per slide. The number of live versus dead cells was averaged and expressed as percent cell survival, i.e., [live cells/(dead + live cells)] × 100.

Comet assay

Comet assay was performed using the Comet Assay Kit (Trevigen, Inc. Gaithersburg, MD) according to the manufacturer's protocol. Briefly, cells were cultured in 6-well plates and treated with CSE or CPT for 6 h. Cells were harvested with trypsin and combined with floating cells in medium containing STI to neutralize the trypsin. Cells were then pelleted and resuspended with cold PBS at 10^5 cells/ml. Fifty microliters of the cell suspension was mixed with 500 μl of LMAgarose, 75 μl of the agarose/cell suspension was pipetted over the sample area of the COMET Slides. The slides were kept flat at 4 °C in a humidity chamber for 30 min, after which they were immersed in cold lysis solution and left at 4 °C overnight. Slides were then transferred into alkali solution and incubated at room temperature for 60 min changing the alkali solution once. Slides were then placed horizontally in an electrophoresis apparatus and electrophoresed at 1 V/cm for 15 min. After fixing with 70% ethanol for 5 min, slides were air-dried and stained with SYBR. Cells were then viewed under epifluorescence microscopy (Nikon Eclipse E800) and photographed with a digital camera (Optronics) at 200× magnification. Data capture was performed using the public domain PC-image analysis program CASP software [17]. The following comet parameters were analyzed: head length (Lhead); tail length (Ltail); comet length (Lcomet); head DNA; tail DNA; tail moment (TM); and olive tail moment (OTM). In addition, apoptotic index was calculated as the percent of cells with diffuse fan-like tails and very small heads from a minimum of three slides counted per condition [17].

Profile of DNA content by flow cytometry

To determine the presence of apoptotic cells, DNA content was measured by flow cytometry as reported previously [16]. Cells were cultured in 6-well plates till confluent. After treatment with CSE or CPT (as a positive control for apoptosis), the medium was harvested to collect floating cells and attached cells were detached from the tissue culture dishes with trypsin/EDTA. Cells were then pelleted together and fixed with 70% ethanol at 4 °C for 30 min. After staining with propidium iodide (50 μg/10^6 cells), cell cycle analysis was performed by flow cytometry. Cells with less DNA staining than that of G1 cells (sub-G1 peaks or A_0 cells) were considered apoptotic.

Transfection of dominant negative AKT (DN-AKT)

Human bronchial epithelial cells were plated into a 6-well plate at a density of 2×10^5/well and transfected with or without DN-AKT using the methods as previously published [Xia, 2008; Liu, 2007]. Briefly, after 24 h culture, cells were transfected with 0.5 μg/well DN-AKT using Lipofectamine 2000 (Invitrogen) for 6 h. After incubating in LHC-9/RPMI overnight, cells were pre-treated with or without HGF (80 ng/ml) followed by exposure to 15%CSE for an additional 6 h. Cells (both floating and attached) were then harvested and used for LIVE/DEAD viability assay or COMET assay as described above.

Measurement of caspases 3, 8 and 9 activities

Caspases 3, 8 and 9 activities were measured with a commercially available colorimetric kit from R&D Systems, following manufacturer's instructions. Briefly, cells were cultured in 60-mm dishes and treated with CSE or CPT for 6 h. Both floating and attached cells were harvested. Cells were collected by centrifugation and suspended in cell lysis buffer (provided by the vendor, R&D Systems, 200 μl/sample). Suspensions were sonicated and centrifuged. The supernatant was then harvested, mixed with reaction buffer, and incubated with the chromogenic peptide substrates for 1 h at 37 °C. The chromogenic activity was determined by spectrophotometry at 405 nm.

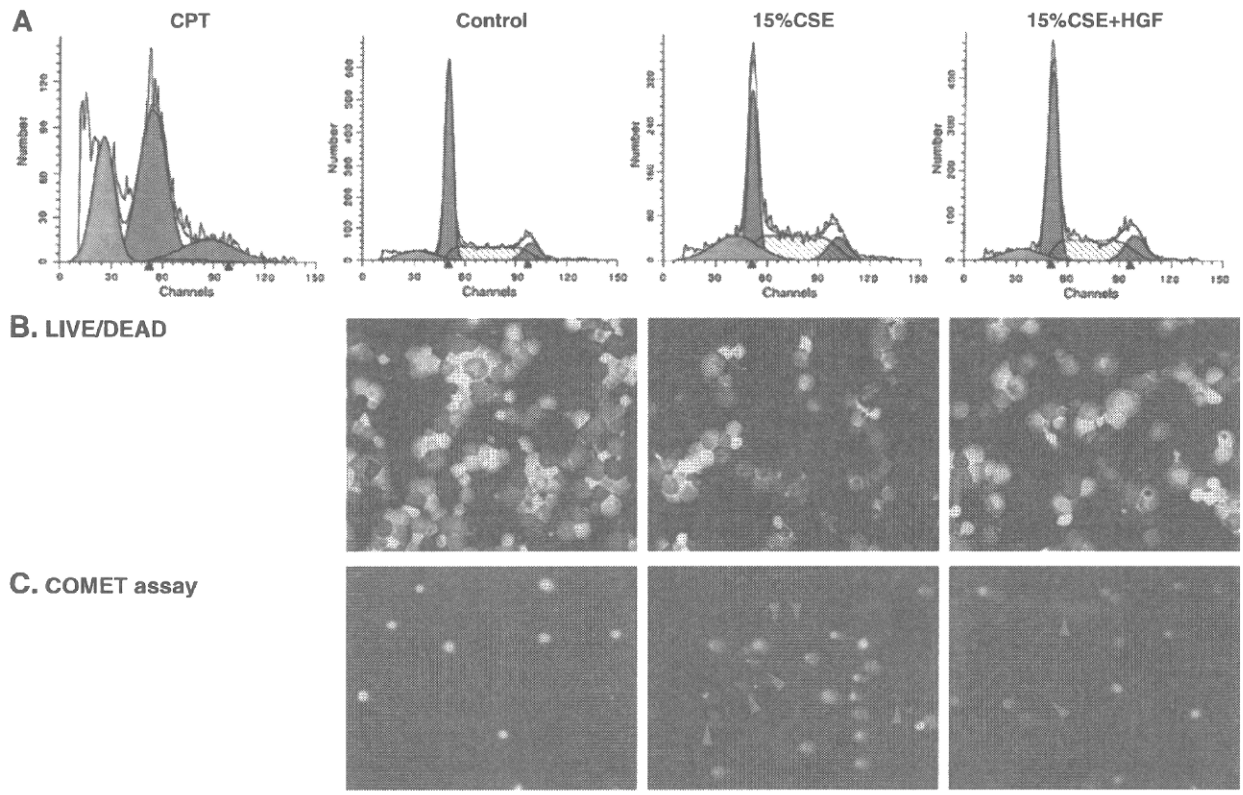

Fig. 1 – HGF inhibits CSE-induced apoptosis of HBECs. Confluent HBECs were incubated with 80 ng/ml HGF for 1 h and then treated with 15% CSE or 1 μM CPT (as a positive control for apoptosis) for 6 h. Cells were then harvested and used for the assessment of apoptosis. Panel A: DNA content was analyzed by flow cytometry. Vertical axis: number of cells; horizontal axis: channel number corresponding to DNA content. Left red peaks: cells with 2N DNA content corresponding to G0, G1 phases; right red peaks: cells with 4N DNA content corresponding to G2, M phases; hatched area: cells corresponding to S phase; blue peak: cells with less than 2N DNA, which were scored as apoptotic. Panel B: cell viability assay by Calcein-AM/EthD staining. Green: alive cells; Red: dead cells. Panel C: COMET assay. Red arrow heads indicate apoptotic cells with fan-like tail and small DNA head. Data presented is one representative from 3 separate occasions. Panel B: quantitative analysis of HGF effect on CSE induced apoptosis by DNA content profiling. Vertical axis: percent of apoptotic cells (%); horizontal axis: treatment with or without CSE. Open bar: control; hatched bar: HGF. Data presented is an average of 3 separate experiments.

Immunoblotting

After treatment with 15% CSE in the presence or absence of HGF, HBEC cell layers were washed with ice cold PBS and homogenized in cell lysis buffer (35 mM Tris–HCl, pH 7.4, 0.4 mM EGTA, 10 mM $MgCl_2$, 1 μM phenylmethylsulfonyl fluoride, 100 μg/ml aprotinin, and 1 μg/ml leupeptin). Samples were then solubilized in sodium dodecyl sulfate (SDS)-polyacrylamide gel (PAGE) sample buffer.

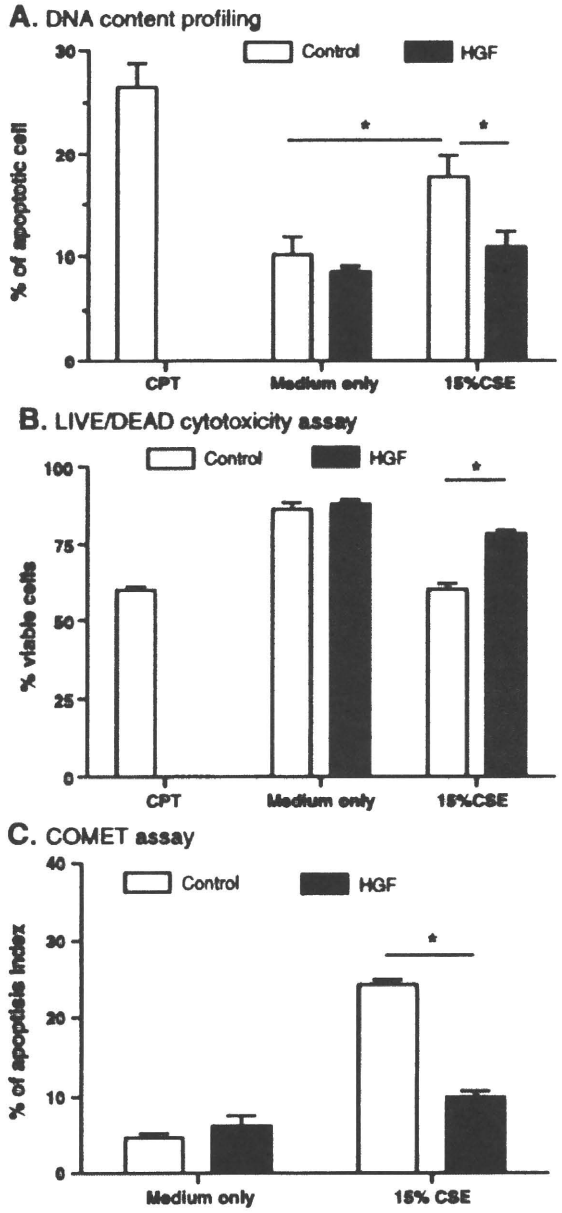

Fig. 2 – Quantitative analysis of HGF effect on CSE induced apoptosis Panel A: DNA content profiling, Vertical axis: percent of apoptotic cells (%); horizontal axis: treatment with or without CSE. Open bar: control; hatched bar: HGF. Panel B: Calcein-AM/EthD staining. Vertical axis: percent of viable cells (%); horizontal axis: treatment with or without CSE. Open bar: control; hatched bar: HGF. Panel C: COMET assay. Vertical axis: percent of apoptotic cells (%) expressed as apoptotic index; horizontal axis: treatment with or without CSE. Open bar: control; hatched bar: HGF. * $p<0.05$. Data presented is one representative from 3 separate occasions.

Table 1 – Analysis of comet assay

	Control	15%CSE	CSE + HGF	p1	p2
L Head	72.0 ± 1.9	46.5 ± 1.1	58.2 ± 1.4	<.0001	<.0001
L tail	18.3 ± 1.8	53.7 ± 3.8	25.7 ± 1.7	<.0001	<.0001
L comet	90.3 ± 2.4	100.3 ± 41	83.9 ± 2.1	0.0377	0.0005
Head DNA	90.7 ± 1.3	50.8 ± 2.1	83.4 ± 1.6	<.0001	<.0001
Tail DNA	9.3 ± 1.3	50.3 ± 1.8	16.6 ± 1.6	<.0001	<.0001
TM	3.4 ± 0.7	29.5 ± 3.2	57 ± 0.8	<.0001	<.0001
OTM	3.3 ± 0	17.8 ± 1.6	5.1 ± 0.3	<.0001	<.0001

p1 = comparison between control vs 15%CSE.
p2 = comparison between 15%CSE vs CSE + HGF.
L: length; TM: tail moment; and OTM: olive tail moment.

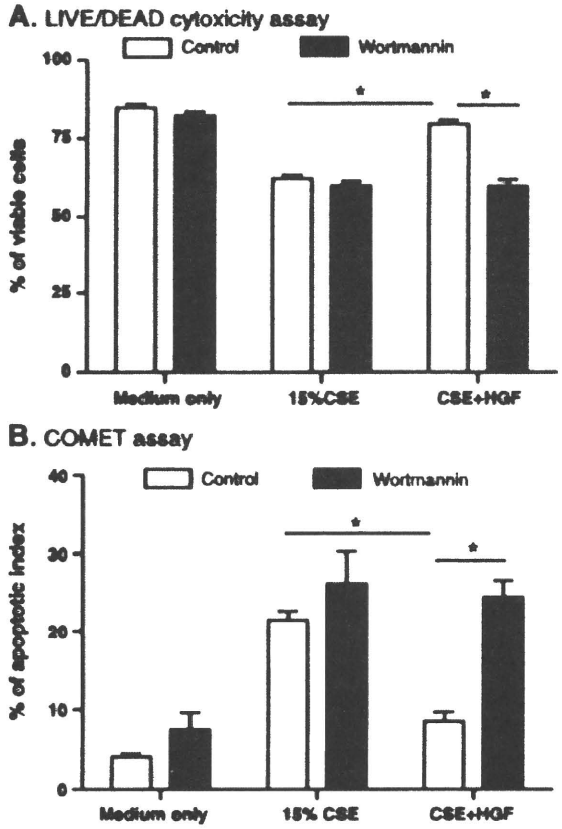

Fig. 3 – Wortmannin attenuates HGF protection of HBEC in response to cigarette smoke exposure. Cultured HBECs were incubated with 10^{-7} M wortmannin, a PI3 kinase inhibitor, for 1 h followed by incubation with or without 80 ng/ml HGF for 1 h. Cells were then incubated with 15% CSE for 6 h. Both floating and attached cells were then harvested. Panel A: Cell viability assay by Calcein-AM/EthD staining. Vertical axis: percent of viable cells (%). Horizontal axis: treatment with or without CSE or HGF. Open bar: control; hatched bar: wortmannin. Panel B: Comet assay. Vertical axis: percent of apoptotic cells (%) expressed as apoptotic index. Horizontal axis: treatment with or without CSE or HGF. Open bar: control; hatched bar: wortmannin. * $p<0.05$.

Equal amounts of protein were loaded into each lane and separated by electrophoresis on 10% SDS-PAGE. After electrophoresis, the separated proteins were transferred to a PVDF membrane (Bio-Rad Laboratories, Hercules, CA). Goat anti-caspase 3 antibody (CPP32), which reacts with both precursor and active forms of human caspase 3, was purchased from R&D Systems (Minneapolis, MN). Primary antibodies against BAD (1:100 dilution; Santa Cruz), Bcl-2 (1:100 dilution; Santa Cruz), Bcl-xL (1:100 dilution; Santa Cruz), phosphorylated BAD (Ser 112, 1:2000 dilution; Cell Signaling, Danvers, MA), XIAP (1:1000 dilution; cell signaling), phosphorylated BAD (Ser 136, 1:1000 dilution, cell signaling), AKT (1:1000 dilution, cell signaling) and phosphorylated AKT (Ser 473 and Thr 308, 1:1000 dilution, cell signaling) were used to detect pro- anti-apoptotic and AKT signaling related protein. Bound antibodies were visualized using peroxidase-conjugated second antibodies and enhanced chemiluminescence (Amersham Biosciences, Buckinghamshire, UK) with a Typhoon Scanner (Amersham Biosciences).

Statistical analysis

Most quantitative data were expressed as mean ± SEM determined from 3 independent experiments unless otherwise indicated. Comparison of paired data was performed using the Student *t*-test, whereas multi-group data were analyzed by ANOVA followed by Tukey correction. $P<0.05$ was considered significant.

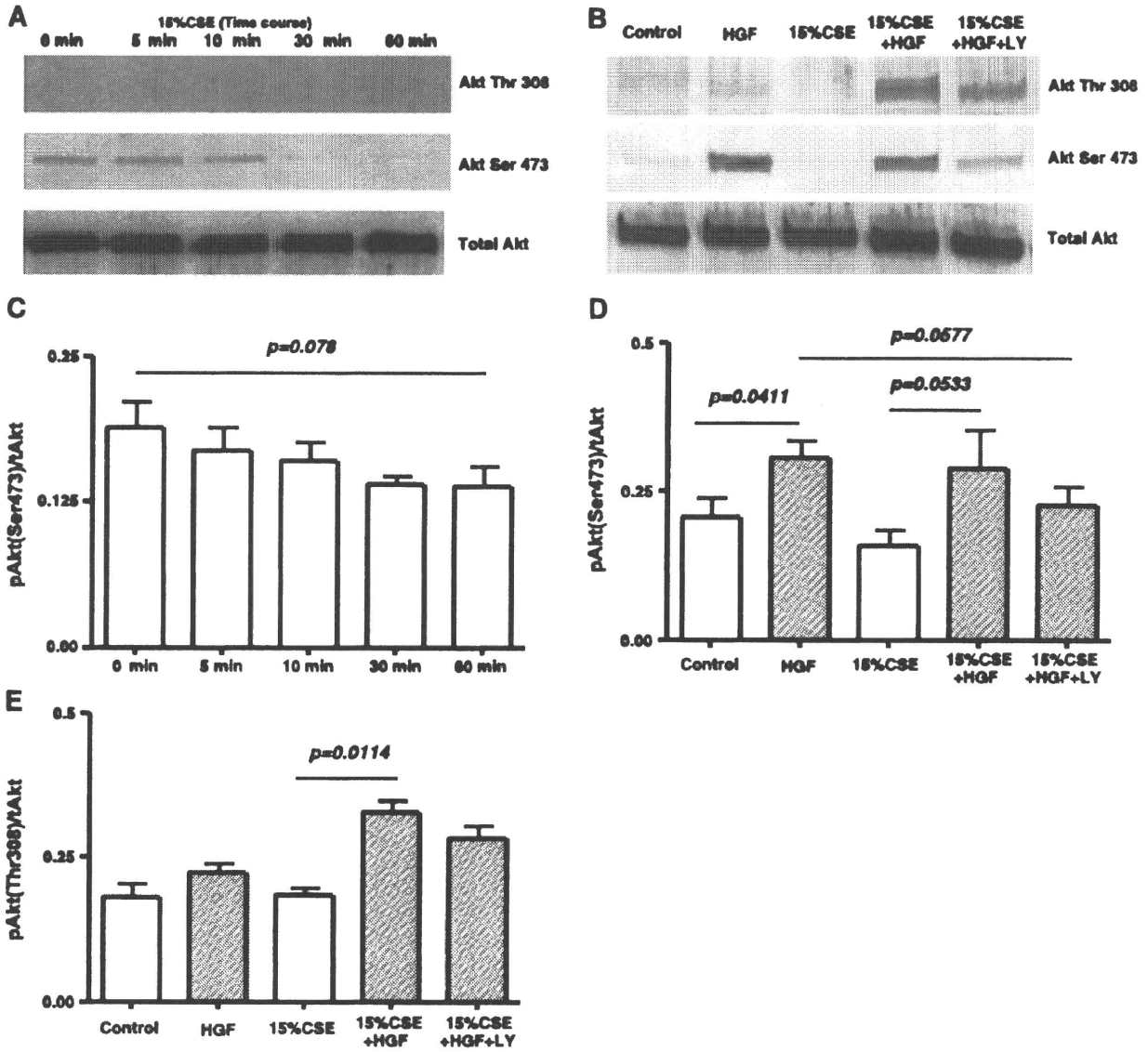

Fig. 4 – Effect of CSE and HGF on AKT phosphorylation. Panel A. Effect of CSE on AKT phosphorylation. Confluent HBEC were exposed to 15%CSE for the time intervals indicated. Cell lysates were immunoblotted for total AKT, phospho-Thr 308 AKT, and phospho-Ser 473 AKT. Panel B: Effect of CSE and LY294002 on HGF-induced AKT phosphorylation. HBECs were incubated with or without the PI3 Kinase inhibitor LY294002 (10^{-6} M) for 1 h followed by incubation with or without HGF for 1 h. The cells were then exposed to 15% CSE for 60 min and harvested for immunoblots. Panels C, D and E: Quantitative density measurement of Panels A and B, respectively. Data presented are the average of 2 independent experiments. P values are as indicated in the figures.

Results

HGF inhibited cigarette smoke-induced apoptosis and cell death in human bronchial epithelial cells

In order to assess the ability of HGF to block CSE-induced apoptosis of HBECs, we first treated the cells with varying concentrations of cigarette smoke extract and found that the effect of CSE on cell viability is concentration dependent. Lower than 10% CSE did not induce significant apoptosis as reported previously [16]. Twenty percent (20%) or higher CSE caused significant necrotic cell death as evidenced by LDH release [18]. Concentration of 15% CSE-induced HBEC apoptosis as evidenced by DNA content profiling, LIVE/DEAD staining and COMET assay (Figs. 1 and 2). Thus, we chose 15% CSE to conduct experiments throughout the current study.

To assess apoptosis, three different methods were used. First, flow cytometric analysis of cellular DNA content was applied to assess apoptotic cell population. By this assessment, it was found that 15%CSE significantly increased the number of cells with hypodiploid DNA (blue color peak, Fig. 1A), indicating apoptosis was induced by 15% CSE ($17.8 \pm 2.1\%$ vs $10.2 \pm 1.6\%$ of control, $p < 0.05$, Fig. 2A). HGF significantly inhibited the induction of apoptosis in response to 15% CSE exposure (Figs. 1A and 2A, $10.8 \pm 1.5\%$ of CSE + HGF, $p < 0.05$). In addition, we had also tried to quantify early apoptosis of the cells by Annexin V/PI staining followed by flow cytometry assay. However, this method gave a false positive result due to the damage of the cell membrane during detachment by trypsine/EDTA. Thus, this assay was not further applied in the current study.

Second, cell viability was assessed using differential staining with calcein acetoxymethylester (calcein-AM, green color) and ethidium homodimer (EthD, red color, Fig. 1B). Consistent with the findings of DNA content profiling, this assay also demonstrated that 15% CSE resulted in cell death, and that HGF significantly reduced cell death in response to 15% CSE exposure (Fig. 2B, $60.2 \pm 2.1\%$ viable cells in CSE-treated vs $78.5 \pm 1.2\%$ in CSE + HGF treated cells, $p < 0.05$).

Third, the COMET single-cell electrophoresis assay demonstrated that 15% CSE caused longer DNA tails and increased the number of cells with small DNA heads and fan-like tails (Fig. 1C). The Apoptotic Index (AI), which is the percentage of cells with a diffuse fan-like tail and a small head, was significantly higher in 15% CSE-treated cells ($24.3 \pm 0.6\%$) than that in the control cells ($4.7 \pm 0.6\%$, $P < 0.05$, Fig. 2C). HGF significantly reduced the cigarette smoke augmentation of the Apoptotic Index ($10.0 \pm 0.8\%$, $P < 0.05$, Fig. 2C). Additional parameters of the comet assay were evaluated in detail by using CASP (Table 1). CSE significantly decreased head length and head DNA, and significantly increased tail length, comet length, tail DNA, tail moment (TM), and olive tail moment (OTM) ($P < 0.05$). HGF reversed these changes significantly ($P < 0.001$).

Role of PI3 kinase and AKT in mediating HGF protection of HBEC in response to CSE exposure

To investigate the signal pathways that mediate HGF protection of HBEC from cigarette smoke-induced apoptosis, the effect of HGF on AKT activation and PI3 kinase was explored. Wortmannin, a potent PI3 kinase inhibitor, partially but significantly inhibited the ability of HGF to preserve HBEC survival in response to cigarette smoke exposure (Figs. 3A and B). We next evaluated AKT phosphorylation. Cigarette smoke inhibits phosphorylation of AKT Ser 473 in a time-dependent manner although it was not statistically significant (Figs. 4A and C). In contrast, HGF-induced phosphorylation of AKT Ser 473 and this was slightly inhibited by cigarette smoke, especially, in the presence of LY294002, a specific PI3 kinase inhibitor (Figs. 4B and D). Interestingly, when cigarette smoke and HGF were added together, a different phosphorylation site, AKT Thr 308, was increased remarkably, while neither HGF nor cigarette smoke alone could induce AKT Thr 308 phosphorylation. Phosphorylation at AKT Thr 308 was slightly suppressed by LY294002 (Figs. 4B and E). Furthermore, the protective effect of HGF on HBEC survival in response to cigarette smoke exposure was suppressed not only by wortmannin (Fig. 3), but also by the transfection of a dominant negative AKT (DN-AKT) into the cells as evidenced by decreased cell viability (Fig. 5A) and increased apoptotic cell number (Fig. 5B).

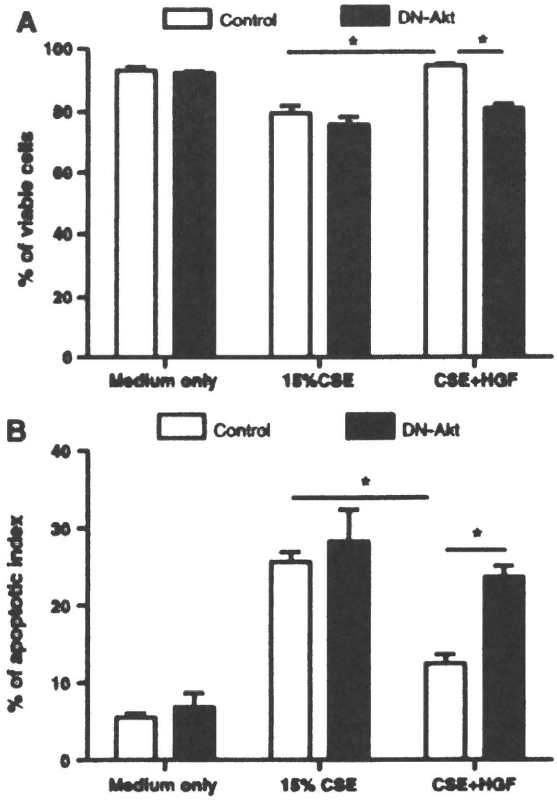

Fig. 5 – Effect of HGF on AKT phosphorylation in the cells transfected with dominant negative AKT (DN-AKT). HBECs were transfected with DN-AKT followed by exposure to 15%CSE as described in the methods. Cell viability (Panel A) and Comet assay (Panel B) were performed. Vertical axis: percent of viable cells (Panel A) or apoptotic index (Panel B); horizontal axis: treatment. Open bar: control cells; hatched bar: cells transfected with DN-AKT. * $p < 0.05$.

Effect of CSE and HGF on the expression of pro-apoptotic and anti-apoptotic proteins

Since caspases are involved in mediating apoptosis, the effect of HGF on the activation of selected caspases was assessed. Cigarette smoke resulted in cleavage of the common effector caspase, caspase 3 (Fig. 6A). This was partially blocked by HGF. Similarly, quantification of caspase activity demonstrated an increase of caspase 3 activity by 15% CSE and its inhibition by HGF (Fig. 6B). Fifteen percent CSE also induced a small increase in the intrinsic effector caspase, caspase 9, and there was a numerical reduction in the presence of HGF, although there was no statistical difference (Fig. 6D). In contrast, the extrinsic effector caspase, caspase 8, was not affected by cigarette smoke or HGF (Fig. 6C).

Next, the effect of HGF and CSE on the expression of selected anti-apoptotic proteins was assessed. Fifteen percent CSE resulted in a time-dependent inhibition of phosphorylation of BAD at serine 136 (Figs. 7A and C). HGF added alone markedly increased BAD phosphorylation (Figs. 7B and D). CSE alone partially blocked HGF-induced phosphorylation of BAD Ser 136 while CSE plus LY294002 (PI3 kinase inhibitor) completely blocked HGF induction of BAD phosphorylation (Figs. 7B and D). Similarly, HGF increased the expression of the anti-apoptotic proteins, Bcl-xL and XIAP and this was significantly inhibited by 15% CSE (Figs. 7E and F).

Discussion

Cigarette smoke exposure results in dose-dependent injury of cultured airway epithelial cells. Relatively low concentrations can induce DNA damage that is repaired [16,19]. Higher concentrations are able to induce apoptosis and necrosis. The current study demonstrates that hepatocyte growth factor (HGF) reduces the sensitivity of airway epithelial cells to cigarette smoke-induced cytotoxicity. Using a concentration of 15% CSE, apoptosis was induced in cultured normal human bronchial epithelial cells as evidenced by COMET assay, DNA content profiling and caspase 3 activation. HGF reduced this apoptosis. The effect of HGF on HBEC survival was mediated by the PI3K/AKT signaling pathway as evidenced by blockage of the HGF effect by an inhibitor of PI3 kinase and a dominant negative AKT, and by demonstrating phosphorylation of downstream AKT. Taken together, these results suggest that HGF can modulate cigarette smoke-induced damage to the airway epithelium, and thus, may contribute to the pathogenesis of cigarette smoke-induced diseases.

Cigarette smoke contains a large number of toxic moieties and likely damages cells through a number of interacting mechanisms. Low concentrations (<10%CSE) of cigarette smoke can induce DNA damage as evidenced by a positive TUNEL assay. This DNA

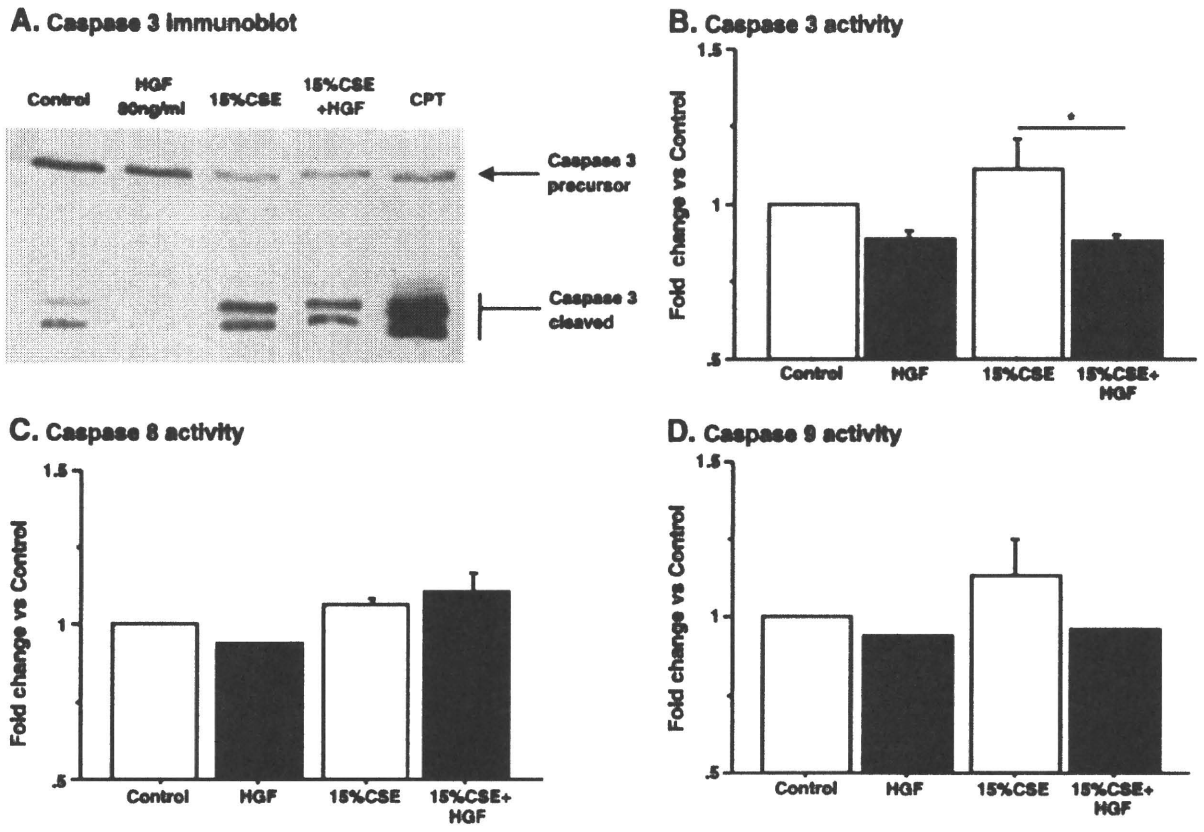

Fig. 6 – Effect of HGF and CSE on caspases 3, 8, and 9 activities. HBECs were incubated with or without HGF for 1 h followed by exposure to 15% CSE for 6 h. Cells were then harvested and assessed for total and cleaved Caspase 3 by immunoblotting (panel A) and for functional activities of caspases 3, 8, and 9. Panel B: caspase 3 activity (n = 4); panel C: caspase 8 activity (n = 3); and panel d: Caspase 9 activity (n = 3). Vertical axes of panels B, C and D: caspase activity expressed as "Fold change vs Control"; horizontal axes: cell treatment. All values are mean ± SEM. *$p < 0.05$; compared with the values of control group.

damage, however, does not lead to cellular apoptosis, but rather to initiation of DNA repair mechanisms [16,19]. If the cigarette smoke is removed, cellular recovery ensues, and cells are able to subsequently proliferate. This process appears to be regulated by cigarette smoke-induced activation of signaling through the STAT3 and NF-κB pathways [12,13]. Interestingly, in these studies, there was no evidence of cigarette smoke-induced activation of signaling through the AKT pathway. The inhibition of apoptosis, which leads to cellular survival following DNA damage [16], and the formation of DNA adducts, which induce the activation of Ras and other mutations [20], are potential means to introduce somatic cell mutations and could, therefore, contribute to the pathogenesis of cancer [21] and, possibly, COPD [1].

Nicotine, a component of cigarette smoke, has been reported to stimulate signaling through the AKT pathway and, as a result, inhibit cellular apoptosis [22,23]. In contrast to the effect of nicotine, cigarette smoke, as noted above, did not activate AKT signaling, a result repeated in the current study. While the

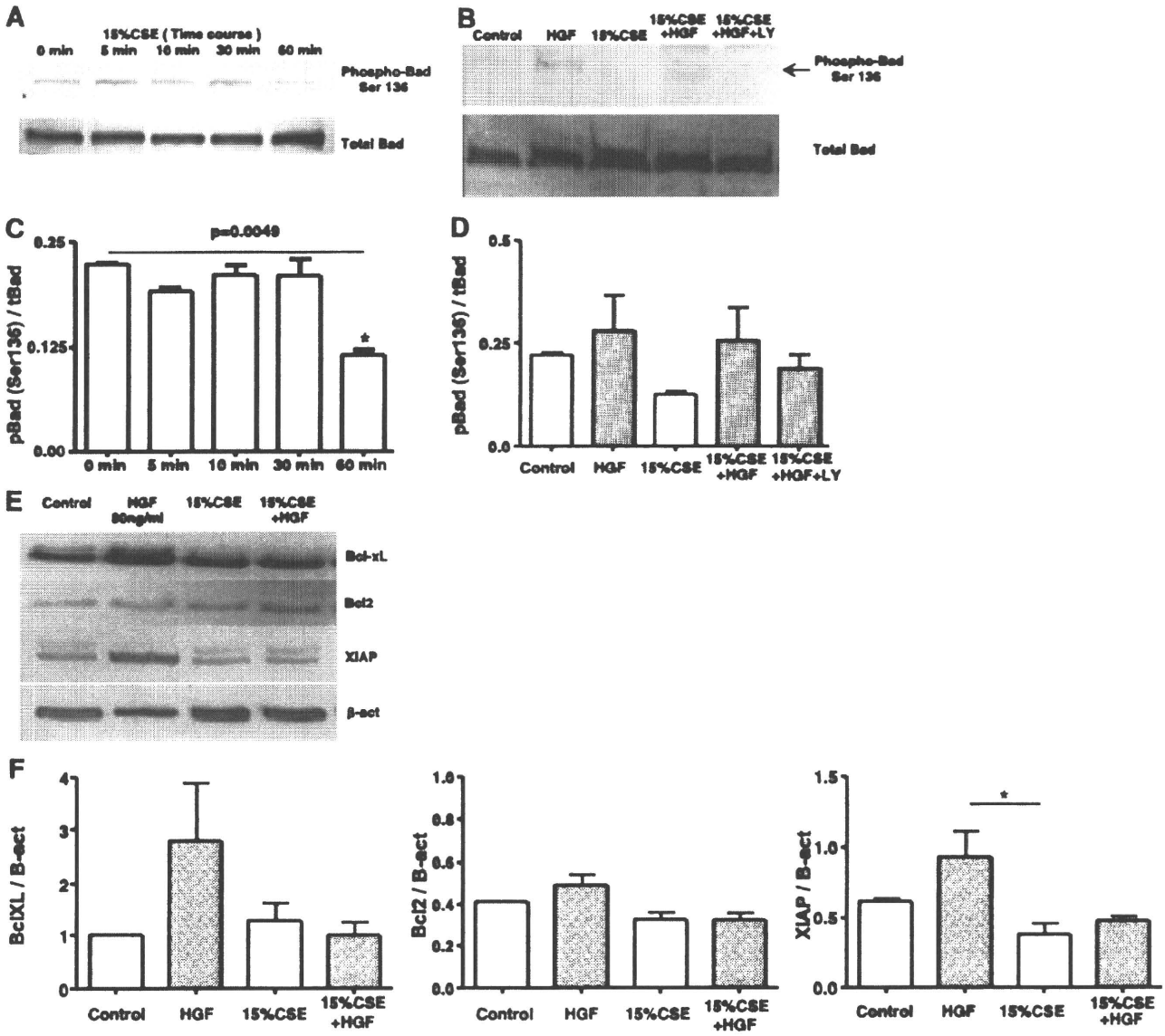

Fig. 7 – Effect of CSE and HGF on anti-apoptotic and pro-apoptotic protein expression. Panels A and C: effect of CSE on BAD phosphorylation. Confluent HBECs were exposed to 15% CSE for varying lengths of time and BAD phosphorylation at Ser 136 was analyzed by immunoblotting (panel A) followed by quantitative analysis using image analysis software (panel C, n = 3). Panels B and D: effect of HGF on CSE inhibition of BAD phosphorylation. HBECs were incubated with or without the PI3 Kinase inhibitor LY294002 (10^{-6} M) for 1 h followed by an incubation with or without HGF for 1 h. The cultures were then exposed to 15% CSE for 60 min. Cells were than harvested and used for western blotting (Panel B). Density of each band was analyzed using image analysis software (panel D, n = 3) Panels E and F: effect of HGF and CSE on expression of selected anti-apoptosis proteins. HBECs were treated as described above and Bcl-2, Bcl-xL, and XIAP were assessed by immunoblotting. A representative result of three replicates is shown in panel E and density of each band was analyzed using image analysis software (panel F, n = 3).

mechanisms for this difference remain undefined, it is possible that other components of cigarette smoke are inhibiting the effect of nicotine. The current study demonstrates, however, that other mediators that signal through AKT, specifically HGF, can inhibit cigarette smoke-induced cytotoxicity. In this regard, HGF alone significantly induced phosphorylation of Akt Ser 473, which was slightly inhibited by CSE. In contrast, neither HGF nor CSE alone could induce Akt Thr 308 phosphorylation. When HGF plus CSE were added, however, Akt Thr 308 was phosphorylated dramatically. These results indicated that HGF and CSE have synergetic effect on Akt Thr 308 phosphorylation and that Akt activation of different sites is stimuli dependent. Consistently, it has been reported that Akt activation is cell type- and stimulus-dependent [24]. LY294002, a specific PI3 kinase inhibitor, could slightly block the phosphorylation of Akt Thr 308 and Akt Ser 473, indicating Akt was activated partially through PI3 kinase pathway in the current study model. While the upstream of Akt other than PI3 kinase remains to be investigated, the current study demonstrated Akt was involved in mediating HGF modulation on HBEC survival in that dominant negative Akt significantly blocked protective effect of HGF.

We have previously shown that low concentrations of cigarette smoke (<10%) lead to DNA damage without cytotoxicity [25]. In this setting, apoptosis is specifically inhibited by an NFkB and STAT3 dependent pathway that leads to activation of PARP and DNA repair. Increasing concentrations lead progressively to apoptosis (15%CSE), which was evaluated in the current study, and necrosis (20%CSE). That the concentration used in the current study was sufficient to induce apoptosis as evidenced by DNA content profiling and COMET assays. The mechanisms by which HGF inhibits apoptosis remain undefined. In retinal pigment epithelial cells, HGF can induce production of anti-oxidants that can protect from apoptosis and, in response to CSE, likely can protect against necrosis as well. In the current study, the effect of HGF on selected proteins related to apoptosis was assessed. Similar to the effect of nicotine that signals through AKT and increases phosphorylation of BAD, the increased levels of phospho BAD were observed when CSE-treated cells were exposed to HGF. Phosphorylated BAD is bound by 14–3–3 proteins and thus is unable to bind to anti-apoptotic Bcl-2 family proteins, and thus, indirectly inhibits apoptosis [26,27]. In contrast, the inhibition of apoptosis in cells exposed to lower concentrations of cigarette smoke [16] was associated with changes in Bcl-xL and XIAP, but changes in these proteins were not observed in the current study although HGF alone did stimulate Bcl-xL and XIAP expressions. This suggests that a number of mechanisms likely modulate the sensitivity of human bronchial epithelial cells to apoptosis. However, it seems that mitochondrial mediated intrinsic apoptosis pathway be involved in mediating CSE-induced apoptosis in that caspase 9 and caspase 3 were activated by CSE but not caspase 8 activity. Further studies such as cytochrome c release assay are required in order to confirm the role of mitochondrial pathway in CSE-mediated HBEC apoptosis. However, this is beyond the scope of the current study and remains to be investigated in the future study.

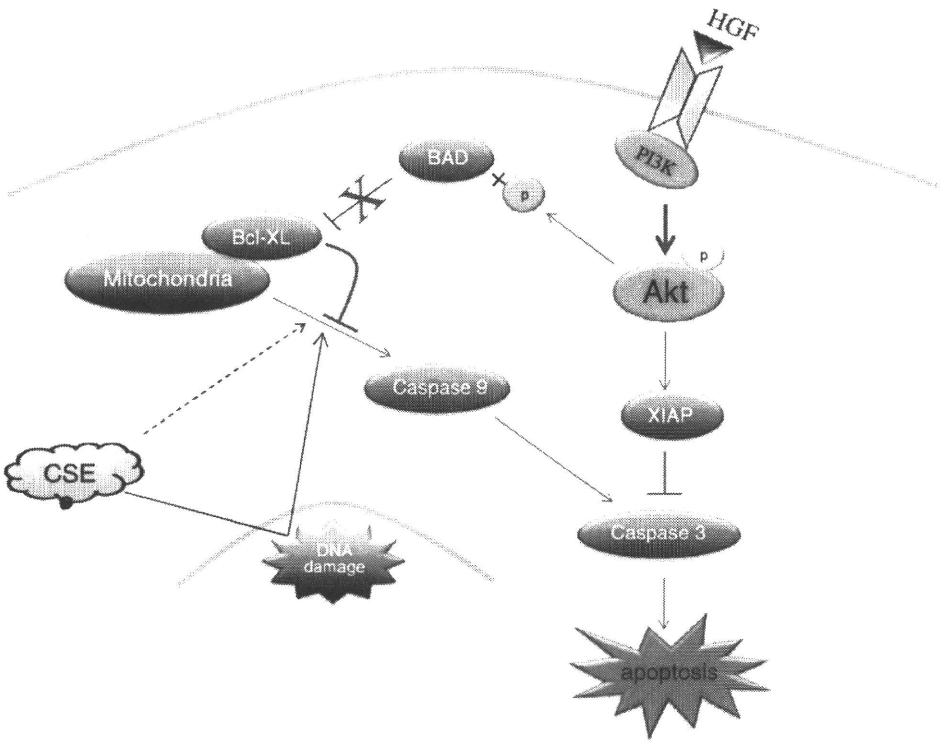

Fig. 8 – Schematic diagram of HGF blockade on CSE-induced apoptosis in HBECs. CSE (15%) directly or indirectly (through inducing DNA damage) activates mitochondrial-caspase 9–caspase 3 pathway. HGF binds to its receptor and activates PI3K/AKT signaling, which stimulates X-linked inhibitor of apoptosis (XIAP) synthesis and induces phosphorylation of BAD. Phosphorylated BAD is incapable of inhibiting Bcl-xL function that inhibits mitochondrial pathway of apoptosis.

The ability of HGF to modulate cellular apoptosis might have a number of effects on cigarette smoke-induced injury in the lung. The inhibition of apoptosis, by preserving lung epithelial cells, could protect the lung from the development of emphysema. In this context, an increased apoptosis has been observed in human lungs from patients with COPD and in a number of animal models [28–30]. The current study supports a direct role for HGF in modulating epithelial cell apoptosis. Indirect effects are also possible, as HGF can stimulate the release of VEGF [31], and deficiencies in VEGF signaling have been associated with emphysema in both human studies and animal models. The ability of HGF to modulate apoptosis in both epithelial and, indirectly, in endothelial cells suggests a coordinated effect on the lung structure.

The inhibition of apoptosis, however, may have significant adverse effects on the lung. Cigarette smoke is notorious for causing DNA damage. One mechanism to protect an organism from the long-term consequences of DNA damage is for cells with DNA damage to undergo apoptosis. As noted above, the ability of cigarette smoke to inhibit apoptosis may contribute to cancer pathogenesis. The ability of HGF to inhibit apoptosis in the presence of cigarette smoke could similarly lead to the accumulation of somatic cell mutations in the face of cigarette smoke exposure. The current study, moreover, suggests that HGF inhibits apoptosis through AKT signaling, a pathway distinct from the mechanisms through which CSE inhibits airway epithelial cell apoptosis. This suggests the possibility of further increases in susceptibility to the accumulation of somatic cell mutations if cigarette smoke exposure is combined with the induction of HGF signaling.

In summary, the current study demonstrates that hepatocyte growth factor (HGF) alters the sensitivity of cultured human bronchial epithelial cells to cigarette smoke-induced cytotoxicity. This effect is mediated through PI3 kinase signaling that activates the AKT signaling pathway as illustrated in Fig. 8. By inhibiting epithelial cell apoptosis, HGF could modulate the response of the lung to injury caused by cigarette smoke. This has the potential to mitigate damage leading to emphysema. Alternatively, HGF signaling could preserve otherwise damaged cells that may lead to the development of cancer or COPD.

REFERENCES

[1] G.P. Anderson, S. Bozinovski, Acquired somatic mutations in the molecular pathogenesis of COPD, Trends Pharmacol. Sci. 24 (2003) 71–76.

[2] E.G. Tzortzaki, N.M. Siafakas, A hypothesis for the initiation of COPD, Eur. Respir. J. 34 (2009) 310–315.

[3] R. Salgia, Role of c-Met in cancer: emphasis on lung cancer, Semin. Oncol. 36 (2009) S52–S58.

[4] N. Puri, R. Salgia, Synergism of EGFR and c-Met pathways, cross-talk and inhibition, in non-small cell lung cancer, J Carcinog 7 (2008) 9.

[5] M.M. Myerburg, J.D. Latoche, E.E. McKenna, L.P. Stabile, J.S. Siegfried, C.A. Feghali-Bostwick, J.M. Pilewski, Hepatocyte growth factor and other fibroblast secretions modulate the phenotype of human bronchial epithelial cells, Am. J. Physiol. Lung Cell. Mol. Physiol. 292 (2007) L1352–L1360.

[6] P. Lassus, J. Janer, C. Haglund, R. Karikoski, L.C. Andersson, S. Andersson, Consistent expression of HGF and c-met in the perinatal lung, Biol. Neonate 90 (2006) 28–33.

[7] S. Padela, J. Cabacungan, S. Shek, R. Belcastro, M. Yi, R.P. Jankov, A.K. Tanswell, Hepatocyte growth factor is required for alveologenesis in the neonatal rat, Am. J. Respir. Crit. Care Med. 172 (2005) 907–914.

[8] Y. Sakamaki, K. Matsumoto, S. Mizuno, S. Miyoshi, H. Matsuda, T. Nakamura, Hepatocyte growth factor stimulates proliferation of respiratory epithelial cells during postpneumonectomy compensatory lung growth in mice, Am. J. Respir. Cell Mol. Biol. 26 (2002) 525–533.

[9] A.E. Hegab, H. Kubo, M. Yamaya, M. Asada, M. He, N. Fujino, S. Mizuno, T. Nakamura, Intranasal HGF administration ameliorates the physiologic and morphologic changes in lung emphysema, Mol. Ther. 16 (2008) 1417–1426.

[10] A. Gazdhar, P. Fachinger, C. van Leer, J. Pierog, M. Gugger, R. Friis, R.A. Schmid, T. Geiser, Gene transfer of hepatocyte growth factor by electroporation reduces bleomycin-induced lung fibrosis, Am. J. Physiol. Lung Cell. Mol. Physiol. 292 (2007) L529–L536.

[11] L. Plantier, S. Marchand-Adam, J. Marchal-Somme, G. Leseche, M. Fournier, M. Dehoux, M. Aubier, B. Crestani, Defect of hepatocyte growth factor production by fibroblasts in human pulmonary emphysema, Am. J. Physiol. Lung Cell. Mol. Physiol. 288 (2005) L641–L647.

[12] X. Liu, STAT3 activation inhibits human bronchial epithelial cell apoptosis in response to cigarette smoke exposure, Biochem. Biophys. Res. Commun. 353 (2007) 121–126.

[13] X. Liu, S. Togo, M. Al-Mugotir, H. Kim, Q. Fang, T. Kobayashi, X. Wang, L. Mao, P. Bitterman, S. Rennard, NF-kappaB mediates the survival of human bronchial epithelial cells exposed to cigarette smoke extract, Respir. Res. 9 (2008) 66.

[14] S.G. Kelsen, I.A. Mardini, S. Zhou, J.L. Benovic, N.C. Higgins, A technique to harvest viable tracheobronchial epithelial cells from living human donors, Am. J. Respir. Cell Mol. Biol. 7 (1992) 66–72.

[15] H. Carp, A. Janoff, Possible mechanisms of emphysema in smokers. In vitro suppression of serum elastase-inhibitory capacity by fresh cigarette smoke and its prevention by antioxidants, Am. Rev. Respir. Dis. 118 (1978) 617–621.

[16] X. Liu, H. Conner, T. Kobayashi, H. Kim, F. Wen, S. Abe, Q. Fang, X. Wang, M. Hashimoto, P. Bitterman, S.I. Rennard, Cigarette smoke extract induces DNA damage but not apoptosis in human bronchial epithelial cells, Am. J. Respir. Cell Mol. Biol. 33 (2005) 121–129.

[17] K. Konca, A. Lankoff, A. Banasik, H. Lisowska, T. Kuszewski, S. Gozdz, Z. Koza, A. Wojcik, A cross-platform public domain PC image-analysis program for the comet assay, Mutat. Res. 534 (2003) 15–20.

[18] S. Carnevali, Y. Nakamura, T. Mio, X. Liu, K. Takigawa, D.J. Romberger, J.R. Spurzem, S.I. Rennard, Cigarette smoke extract inhibits fibroblast-mediated collagen gel contraction, Am. J. Physiol. 274 (1998) L591–L598.

[19] H. Kim, X. Liu, T. Kobayashi, H. Conner, T. Kohyama, F.Q. Wen, Q. Fang, S. Abe, P. Bitterman, S.I. Rennard, Reversible cigarette smoke extract-induced DNA damage in human lung fibroblasts, Am. J. Respir. Cell Mol. Biol. 31 (2004) 483–490.

[20] J.I. Kim, J.T. Suh, K.U. Choi, H.J. Kang, D.H. Shin, I.S. Lee, T.Y. Moon, W.T. Kim, Inactivation of O6-methylguanine-DNA methyltransferase in soft tissue sarcomas: association with K-ras mutations, Hum. Pathol. 40 (2009) 934–941.

[21] D.M. DeMarini, Genotoxicity of tobacco smoke and tobacco smoke condensate: a review, Mutat. Res. 567 (2004) 447–474.

[22] K.A. West, J. Brognard, A.S. Clark, I.R. Linnoila, X. Yang, S.M. Swain, C. Harris, S. Belinsky, P.A. Dennis, Rapid Akt activation by nicotine and a tobacco carcinogen modulates the phenotype of normal human airway epithelial cells, J. Clin. Invest. 111 (2003) 81–90.

[23] P. Dasgupta, R. Kinkade, B. Joshi, C. Decook, E. Haura, S. Chellappan, Nicotine inhibits apoptosis induced by chemotherapeutic drugs by up-regulating XIAP and survivin, Proc. Natl Acad. Sci. USA 103 (2006) 6332–6337.

[24] Y. Kawakami, H. Nishimoto, J. Kitaura, M. Maeda-Yamamoto, R.M. Kato, D.R. Littman, M. Leitges, D.J. Rawlings, T. Kawakami, Protein kinase C betaII regulates Akt phosphorylation on Ser-473 in a cell type- and stimulus-specific fashion, J. Biol. Chem. 279 (2004) 47720–47725.

[25] J.C. Strefford, T.M. Lane, A. Hill, L. LeRoux, N.J. Foot, J. Shipley, R.T. Oliver, Y.J. Lu, B.D. Young, Molecular characterisation of the t (1;15)(p22;q22) translocation in the prostate cancer cell line LNCaP, Cytogenet. Genome Res. 112 (2006) 45–52.
[26] J. Zha, H. Harada, E. Yang, J. Jockel, S.J. Korsmeyer, Serine phosphorylation of death agonist BAD in response to survival factor results in binding to 14-3-3 not BCL-X(L), Cell 87 (1996) 619–628.
[27] X.M. Zhou, Y. Liu, G. Payne, R.J. Lutz, T. Chittenden, Growth factors inactivate the cell death promoter BAD by phosphorylation of its BH3 domain on Ser155, J. Biol. Chem. 275 (2000) 25046–25051.
[28] J.L. Wright, A. Churg, Animal models of cigarette smoke-induced COPD, Chest 122 (2002) 301S–306S.
[29] N.F. Voelkel, C.D. Cool, Pulmonary vascular involvement in chronic obstructive pulmonary disease, Eur. Respir. J. Suppl. 46 (2003) 28s–32s.
[30] M. Plataki, E. Tzortzaki, P. Rytila, M. Demosthenes, A. Koutsopoulos, N.M. Siafakas, Apoptotic mechanisms in the pathogenesis of COPD, Int J Chron Obstruct Pulmon Dis 1 (2006) 161–171.
[31] G. Dong, Z. Chen, Z.Y. Li, N.T. Yeh, C.C. Bancroft, C. Van Waes, Hepatocyte growth factor/scatter factor-induced activation of MEK and PI3K signal pathways contributes to expression of proangiogenic cytokines interleukin-8 and vascular endothelial growth factor in head and neck squamous cell carcinoma, Cancer Res. 61 (2001) 5911–5918.

Allergology International. 2010;59:363-367
DOI: 10.2332/allergolint.10-OA-0197

ORIGINAL ARTICLE

Reference Ranges for Exhaled Nitric Oxide Fraction in Healthy Japanese Adult Population

Kazuto Matsunaga[1], Tsunahiko Hirano[1], Tomotaka Kawayama[2], Takahiro Tsuburai[3], Hiroyuki Nagase[4], Hisamichi Aizawa[2], Kazuo Akiyama[3], Ken Ohta[4] and Masakazu Ichinose[1]

ABSTRACT

Background: The measurement of the exhaled nitric oxide fraction (FENO) is proposed as a useful marker of airway inflammation. In healthy adults, there have been a few studies of the reference ranges for FENO in Caucasians. A community study in other regions may reveal any possible ethnic differences in the FENO levels.

Methods: A total of 240 healthy adults aged between 18 to 74 years were recruited from four medical centers in Japan. Current smokers and subjects having a history of atopic disease were not included. FENO was measured using an online electrochemical nitric oxide analyzer according to the current guidelines. The reference ranges for FENO were estimated using two different statistical methods recommended by International Federation of Clinical Chemistry and Laboratory Medicine.

Results: The mean FENO was 16.9 ppb (parts per billion) with a 95% prediction interval (2.5 to 97.5 percentiles) of 6.5 to 35.0 ppb in healthy Japanese adults. Normality assumptions were met for the logarithm-transformed FENO. The geometric mean FENO was 15.4 ppb with a mean ± two standard deviations of 6.5 to 36.8 ppb. Age, gender, height, and past smoking history were not associated with the FENO levels.

Conclusions: The reference ranges for FENO in healthy Japanese adults were similar to those of Caucasians. It seems reasonable that the upper limit of FENO for healthy adults should be set at approximately 36.0 ppb irrespective of ethnic differences.

KEY WORDS

airway inflammation, asthma, atopy, ethnic difference, smoking

ABBREVIATIONS

BMI, Body mass index; FENO, Exhaled nitric oxide fraction; ppb, Parts per billion.

INTRODUCTION

The measurement of the exhaled nitric oxide fraction (FENO) has been proposed as a useful marker of airway inflammation.[1] FENO levels are elevated in inflammatory lung diseases, such as asthma.[1-3] Establishing reference ranges in healthy subjects would be useful for the interpretation of FENO measurements. Although the measurement procedures have been standardized, the normal upper limits of FENO levels have not been specified.[1]

Previous studies have demonstrated that there are several determinants of FENO, such as age, gender, atopy, smoking status, and diet.[1,4-17] It has been reported that the FENO levels in Asian children are significantly higher than those in Caucasian child ren.[15-17] However, in healthy adults, there have been a few studies of the reference ranges for FENO in Caucasians.[4-6] A community study in other regions may reveal any possible ethnic differences in the FENO levels.

In the present study, the reference ranges for FENO in healthy Japanese adults were estimated using two different statistical methods recommended

[1]Third Department of Internal Medicine, Wakayama Medical University, Wakayama, [2]Department of Medicine, Kurume University, Fukuoka, [3]Clinical Research Center for Allergy and Rheumatology, National Hospital Organization, Sagamihara National Hospital, Kanagawa and [4]Department of Medicine, Teikyo University, Tokyo, Japan.
Correspondence: Masakazu Ichinose, MD, PhD, Third Department of Internal Medicine, Wakayama Medical University, School of Medicine, 811-1 Kimiidera, Wakayama 641-8509, Japan.
Email: masakazu@wakayama-med.ac.jp
Received 23 February 2010. Accepted for publication 13 April 2010.